Tutorial: Measurement of fluorescence spectra and determination of relative fluorescence quantum yields of transparent samples

Marcia Levitus. School of Molecular Sciences and The Biodesign Institute. Arizona State University, Tempe, AZ, USA.

Abstract

The measurement of fluorescence spectra and the determination of fluorescence quantum yields in transparent samples are conceptually simple tasks, but these procedures are subject to several pitfalls that can lead to significant errors. Available technical reports and protocols often assume that the reader possesses a solid theoretical background in spectroscopy and has ample experience with fluorescence instrumentation, but this is often not the case given the many applications of fluorescence in diverse fields of science. The goal of this tutorial is to provide a didactic treatment of the topic that will hopefully be accessible to readers without extensive expertise in the field of fluorescence. The article covers the theoretical background needed to understand the origins of the most common artifacts researchers can expect. Possible artifacts are illustrated with examples to help readers avoid them or identify them if present. A step-by-step example of a fluorescence quantum yield determination in solution is provided with detailed experimental information to help readers understand how to design and analyze experiments.

1 Introduction

The popularity of fluorescence-based techniques in fields spanning materials to biology continues to grow with the ever-increasing developments in single-molecule detection and super-resolution microscopy [1–5]. The brightness of a fluorophore at a particular excitation wavelength (λ_{Ex}) , which in general terms measures the ability of a molecule to emit light via photo-excitation, is commonly defined as the product of the molar absorption coefficient $(\epsilon(\lambda_{Ex}))$ and the fluorescence quantum yield (ϕ_f) [6]. The fluorescence quantum yield is the fraction of absorbed photons that are emitted as fluorescence, so this parameter is one of the factors that determine the number of photons that can be detected experimentally and it is therefore intimately related to the limit of detection in fluorescence spectroscopy. Hence, the experimental determination of ϕ_f is a critical step in the characterization of fluorescent molecules and materials. Moreover, accurate determinations of ϕ_f are needed for the quantitative interpretation of FRET (Förster resonance energy transfer) data. FRET is a popular tool in the biosciences that is commonly used to measure inter-molecular distances [3, 7]. Fluorescent donor and acceptor probes for FRET are often extrinsic fluorophores attached to amino acids and nucleobases. The determination of the donor-acceptor distance requires

previous knowledge of a parameter known as Förster's distance (R_0 , defined as the donor-acceptor distance that results in 50 % energy transfer efficiency), which depends on the fluorescence quantum yield of the donor [8–10]. Although R_0 values are easy to find in websites and textbooks, these values are most commonly calculated from ϕ_f values measured in solution. Fluorescence quantum yields are often affected by the dye's environment (e.g. polarity, viscosity, pH, and specific interactions with amino acids or nucleobases) [8, 9, 11], so the rigorous interpretation of FRET data requires the experimental determination of ϕ_f (and therefore R_0) for the probes incorporated in the biomolecules of interest.

Conceptually, the determination of the fluorescence quantum yield of a transparent sample is relatively simple. Yet, the accurate determination of ϕ_f is surprisingly challenging. This tutorial aims to provide readers with the tools necessary to carry out accurate relative quantum yield determinations in transparent samples. There are many excellent technical reports and protocols that describe proper experimental procedures and recommended standards [12–15], but these sources assume that readers have expertise with fluorescence theory and instrumentation. The goal of this tutorial is to provide a didactic treatment of the topic that will hopefully be accessible to readers with little expertise in the field of fluorescence. Readers seeking complementary information or a more thorough theoretical background are encouraged to read the textbooks by J. R. Lakowicz [8], B. Valeur and M. Berberan-Santos [9], and D. Jameson [16].

2 Background

State diagrams such as the one shown in Fig. 1A (frequently called Jablonski diagrams) are commonly used to depict molecular states and photophysical processes. Thick horizontal lines represent molecular electronic states while thin lines represent vibrational states. Solid arrows are used to indicate radiative processes (absorption and emission), and wavy arrows indicate nonradiative transitions. With very few exceptions, the lowest electronic state of an organic molecule is a singlet state (labeled as S_0 in Fig. 1A). In a typical fluorescence experiment, a light source such as a laser or a lamp is used to excite a molecule to the first electronic excited state (denoted by S_1). Transitions to different vibrational states within the first electronic excited state are allowed (see (1) in Fig. 1A), but in solution, molecules relax rapidly (in picoseconds) to the lowest vibrational level of the first electronic excited state by transferring excess vibrational energy to the solvent molecules (vibrational relaxation, (2) in Fig 1A). Further relaxation to the ground state occurs over longer timescales, usually tens of picoseconds to hundreds of nanoseconds, depending on the molecule and conditions. Emission of photons accompanying the relaxation of the first electronic excited state to the ground state is called fluorescence (See (3), Fig. 1A). Importantly, S_1 can be depopulated by other mechanisms that do not involve the emission of light (non-radiative processes), and accordingly, only a fraction of the absorbed photons results in emission of fluorescence photons. Non-radiative processes include internal conversion, intersystem crossing to the triplet state, energy transfer to another molecule, etc. Readers interested in learning more about the nature of the different non-radiative mechanisms that lead to the relaxation of electronic excited states are encouraged to read references [9,17]. Because the focus of this article is fluorescence emission, we will consider all other deactivation mechanisms collectively and focus on the efficiency of fluorescence emission relative to all non-radiative paths combined.

For a given photon absorption event, the fate of the excited state depends on the relative kinetic rates of the different processes that deactivate the excited state. One can envision the fate of an excited state as a random event with many outcomes: fluorescence, internal conversion, intersystem crossing, or some other non-radiative process (Fig. 1B). The probability of each outcome depends on how the rate of that particular process compares to the rates of all deactivation processes combined. For instance, the probability that the singlet excited state will deactivate by emission of a photon, i.e. fluorescence, is given by the rate of fluorescence emission (k_f) divided by the sum of the rates of all the processes that contribute to the deactivation of the excited state $(k_f + \Sigma k_{nr})$, where the sum combines all non-radiative processes).

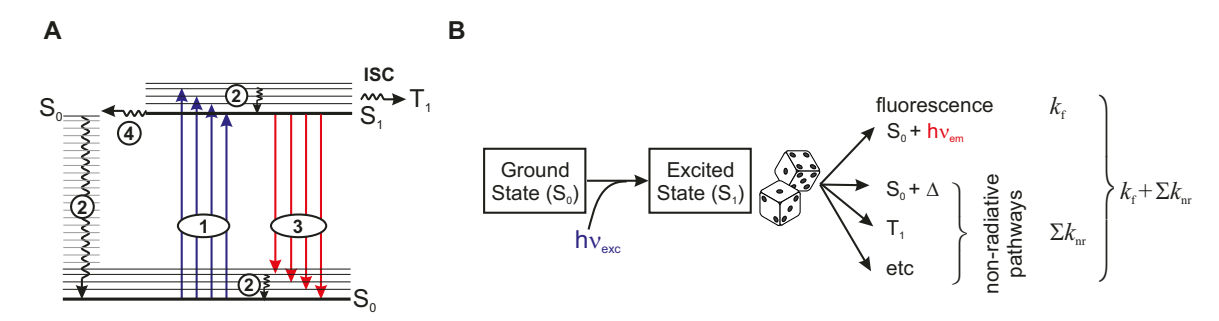


Figure 1: A Simplified Jablonski diagram depicting molecular states and photophysical processes. Only the first singlet excited state (S_1) , and only a few vibrational states are shown for clarity. Absorption ① and Fluorescence ③ are radiative processes, depicted in blue and red, respectively. Vibrational relaxation is indicated with wavy vertical arrows, ②. Internal conversion, ④, is an isoenergetic nonradiative transition between the lowest vibrational level of S_1 and an excited vibrational state of S_0 (note that the higher energy vibrational states of S_0 are shown only on the left-side of the figure for clarity). Internal conversion is followed by vibrational relaxation within the S_0 manifold, ② . ISC denotes intersystem-crossing, a radiationless process that leads to the creation of the triplet state. B Cartoon depiction of the possible pathways by which the first excited state can deactivate, highlighting the random nature of the process. The probability that the excited state deactivates via fluorescence is given by the ratio of k_f to $k_f + \Sigma k_{nr}$, where Σk_{nr} represents the sum of the rate constants of all the non-radiative pathways that can deactivate S_1 . The symbol Δ represents heat (vibrational energy).

The fluorescence quantum yield, ϕ_f , is the quantity that measures the probability that the excited state of a molecule will deactivate to the ground state with emission of a photon. A value of $\phi_f = 0.8$, for example, indicates that the molecule will deactivate with emission of fluorescence with 80% probability, leaving the remaining 20% probability to all other decay mechanisms combined. If a single molecule were excited continuously, this probability translates into an average of 80 emitted photons per 100 photons absorbed. This definition establishes the basis for the optical measurement of the fluorescence quantum yield: ϕ_f is the number of photons emitted as fluorescence (N_f) over a given time period, divided by the

number of photons that were absorbed (N_A) :

$$\phi_f = \frac{N_f}{N_A} \tag{1}$$

From a practical perspective, the measurement of N_f would require the detection of all emitted photons, which cannot be achieved using conventional fluorescence spectrometers because these instruments are designed to detect only a fraction of the emitted light. We should note that the absolute measurement of a fluorescence quantum yield can be achieved using instruments equipped with an integrating sphere detector [18,19]. Absolute measurements ϕ_f are gaining popularity, but integrating spheres are still considered sophisticated accessories and are not widespread. For this reason, in this tutorial we will focus on the optical determination of relative fluorescence quantum yields, which can be accomplished with conventional spectrofluorimeters readily available to most researchers. In brief, relative measurements rely on the comparison between the fluorescence signal from the sample of interest and the signal from a sample of known ϕ_f . If the sample and reference are measured under the same conditions, the same (unknown) fraction of the emitted photons will be measured in both cases, allowing the determination of one fluorescence quantum yield relative to the other (see below).

In addition to optical methods, which rely on the detection of the emitted photons, fluorescence quantum yields can also be determined indirectly by measuring the amount of excitation energy that is converted into heat and dissipated into the solvent. Examples of calorimetric methods are thermal lensing and photoacoustic spectroscopy, and readers interested in these techniques are referred to references [20–23].

As stated above, ϕ_f is the number of photons emitted as fluorescence divided by the number of photons absorbed (Eq. 1). We have already established that conventional spectrofluorimeters are not able to measure the total number of the emitted photons (N_f) , but only an unknown fraction k determined by a series of factors that include the solid angle through which the instrument collects light, the transmission efficiency of various optical components, and the quantum efficiency of the detector. Therefore, the number of photons detected by the instrument is $N_{f,d} = kN_f$. As it will become evident as we progress through this tutorial, attempting to characterize this fraction is far from straightforward due to the many factors that contribute to it. This limitation is circumvented by performing an experiment with a reference sample of known ϕ_f in conditions that ensure that the fraction of photons detected for the unknown sample (S) and the reference (R) remains the same. Under these conditions, the ratio of the number of photons detected for the sample and reference $(N_{f,d}^S/N_{f,d}^R)$ equals the ratio of the number of photons emitted (N_f^S/N_f^R) , and we can write

$$\frac{\phi_f^S}{\phi_f^R} = \frac{N_f^S/N_A^S}{N_f^R/N_A^R} = \frac{N_{f,d}^S/N_A^S}{N_{f,d}^R/N_A^R} \tag{2}$$

Eq. 2 seems straightforward, but we still need to relate the variables involved in the equation $(N_{f,d}, N_A)$ with quantities that can be easily measured using conventional spectrophotometers and spectrofluorimeters. Spectrophotometers measure the absorbance of the

sample, which is related to the fraction of the incident light that is transmitted by the sample (i.e. the transmittance). Most commonly, spectrofluorimeters measure an electric signal in arbitrary units that is proportional to the number of photons detected at the wavelength determined by the emission monochromator of the instrument. Our next step is therefore to describe the relationship between the experimental observables (absorbance and fluorescence intensity) and the variables involved in the calculation of ϕ_f^S/ϕ_f^R (N_A and $N_{f,d}$, Eq. 2).

Let us first focus on the quantity $N_{f,d}$. When the fluorescence intensity of a sample is recorded using a spectrofluorimeter, the sample is continuously excited by the excitation source (usually a lamp) and molecules experience large numbers of successive excitation-emission cycles. Photons emitted as fluorescence have a distribution of energies (and therefore wavelengths) that reflect the probability of the various transitions from the lowest vibrational level of the first excited electronic state to different vibrational levels of the ground state. This energy distribution defines the fluorescence spectrum (often called the emission spectrum) of the compound, which can be measured using a conventional spectrofluorimeter.

In practice, the fluorescence intensity is measured at a given combination of excitation and emission wavelengths, λ_{Ex} and λ_{Em} , respectively. To acquire the entire fluorescence spectrum, the instrument is set at a given λ_{Ex} value and λ_{Em} is scanned to cover the whole fluorescence spectrum. As mentioned above, not all emitted photons are detected; the instrument collects fluorescence over a given solid angle, only a fraction of the photons collected is transmitted through the optical components of the detection system, and finally, only a fraction of the photons that reach the detector generates an electric response. As a consequence, the total number of photons detected is only a fraction of the number of photons emitted by the sample at all wavelengths, $(N_f$ in Eq. 1). Let us define the fluorescence intensity, $I_f(\lambda_{Ex}, \lambda_{Em})$, as the number of photons detected at wavelength λ_{Em} , so that the integral of the measured spectrum, $\int_0^\infty I_f(\lambda_{Ex}, \lambda_{Em}) d\lambda_{Em}$ represents the total number of detected photons including all wavelengths $(N_{f,d})$. Using the definition of ϕ_f (Eq. 1), we can write:

 $\int_{0}^{\infty} I_f(\lambda_{Ex}, \lambda_{Em}) d\lambda_{Em} = kN_f = kN_A \phi_f \tag{3}$

where the limits of integration indicate that all photons emitted should be counted regardless of their energy. In practice, as discussed in section 4.2.7, integration is performed over a finite wavelength range. The constant k in Eq. 3 represents the fraction of all emitted fluorescence photons that are detected, and so far, we have assumed that this quantity does not depend on emission wavelength. However, as we will discuss in section 3, this is never the case. The transmission efficiency of the diffraction gratings used in the monochromators of most instruments and the response of the photomultiplier tubes used as detectors are both wavelength-dependent, and therefore the fraction of photons detected is not constant across the fluorescence spectrum. The quantity $I_f(\lambda_{Ex}, \lambda_{Em})$ in Eq. 3 is therefore not the measured fluorescence intensity, but a fluorescence intensity that has been obtained after correcting the measured value for the wavelength-dependent efficiency of the detection system. Section 3 describes the experimental considerations and corrections needed to obtain the corrected spectrum that should be used in Eq. 3.

We will next turn our attention to the quantity N_A . The number of photons absorbed

during the experiment depends on the absorbance of the solution at the excitation wavelength used to acquire the fluorescence spectrum (λ_{Ex}) . Indeed, the absorbance of the sample defines a relationship between the intensity of the incident light, $I_0(\lambda_{Ex})$, and the intensity absorbed by the sample, $I_A(\lambda_{Ex})$:

$$I_A(\lambda_{Ex}) = I_0(\lambda_{Ex})(1 - 10^{-A(\lambda_{Ex})})$$
(4)

To derive Eq. 4, we used the definition of absorbance $(A = -\log(I_T/I_0))$, and the fact that the absorbed intensity is the difference between the intensity of the incident light and the intensity of the transmitted light $(I_A(\lambda_{Ex}) = I_0(\lambda_{Ex}) - I_T(\lambda_{Ex}))$. Therefore, the term $(1 - 10^{-A(\lambda_{Ex})})$ represents the fraction of the incident photons that are absorbed by the sample at a given excitation wavelength. The number of photons absorbed by a solution can then be expressed as $N_A(\lambda_{Ex}) = N_0(\lambda_{Ex})(1 - 10^{-A(\lambda_{Ex})})$, where N_0 is the number of incident photons.

Eq. 3 can be now written as

$$\int_0^\infty I_f(\lambda_{Ex}, \lambda_{Em}) d\lambda_{Em} = kN_0 (1 - 10^{-A(\lambda_{Ex})}) \phi_f$$
 (5)

The numerical value of the proportionality constant k is generally unknown and depends on a large number of instrumental conditions that are hard to quantitate and reproduce. Therefore, the value of the measured intensity has no real meaning, and it is generally expressed in arbitrary units. However, if the fluorescence spectra of the sample and the reference are acquired using identical experimental conditions (including excitation wavelength, cuvette size and geometry, slit bandwidths, etc), the values of k and $N_0(\lambda_{Ex})$ can be regarded as equal and the ratio of the integrated corrected emission spectra can be expressed as

$$\frac{\int_0^\infty I_f^S(\lambda_{Ex}, \lambda_{Em}) d\lambda_{Em}}{\int_0^\infty I_f^R(\lambda_{Ex}, \lambda_{Em}) d\lambda_{Em}} = \frac{(1 - 10^{-A^S(\lambda_{Ex})}) \phi_f^S}{(1 - 10^{-A^R(\lambda_{Ex})}) \phi_f^R}$$
(6)

We stress that Eq. 6 was derived under the assumption that the two measurements (i.e. the sample and reference emission scans) capture the same fraction of the emitted light. This is in part determined by the solid angle through which the instrument collects light, which depends on the refractive index of the solvent (n). The light emitted as fluorescence refracts at the surfaces separating the solution, the cuvette, and air, and consequently the fluorescence flux that falls on the aperture of the detection channel of the instrument depends on the refractive index of the solvent [8, 24]. If the solvents used to prepare the reference and sample solutions have different refractive indices, the fraction of photons collected in the two experiments can be significantly different. To correct for this difference, a correction factor that depends on the square of the refractive indices must be included in Eq. 6, which written in terms of ϕ_f^S/ϕ_f^R becomes:

$$\frac{\phi_f^S}{\phi_f^R} = \frac{n_S^2}{n_R^2} \times \frac{\int_0^\infty I_f^S(\lambda_{Ex}, \lambda_{Em}) d\lambda_{Em}}{\int_0^\infty I_f^R(\lambda_{Ex}, \lambda_{Em}) d\lambda_{Em}} \times \frac{(1 - 10^{-A^R(\lambda_{Ex})})}{(1 - 10^{-A^S(\lambda_{Ex})})}$$
(7)

The values of n for common solvents are listed in the Supplemental Information File.

We note that the ratio $\frac{(1-10^{-A^S(\lambda_{Ex})})}{(1-10^{-A^R(\lambda_{Ex})})}$ is often approximated by the ratio $\frac{A^S(\lambda_{Ex})}{A^R(\lambda_{Ex})}$, and while the approximation may not result in a significant error at the low absorbance values used in the experiments (typically A < 0.04, see below), the calculation of the term $(1-10^{-A^S(\lambda_{Ex})})$ in Eq. 7 is straightforward and is always preferred. An explanation of the origin of this approximation is provided in the Supplemental Information File (see section S2). In addition, a common misconception is that the calculation of ϕ_f^S requires comparing the fluorescence output of the sample with a reference of equal concentration. Eq. 7 shows that the only variable of interest is the absorbance of the solution, which can be measured directly with a conventional spectrophotometer. The absorbance of the solution is of course related to the concentration of fluorophores as described by Beer-Lambert's law, but it also depends on the extinction coefficient of the compound at the wavelength of excitation. The fluorescence intensity of a solution of a fluorescent compound will be negligible if excited at a wavelength where the compound does not absorb (small extinction coefficient), regardless of its concentration.

Eq. 7 is the basis for the measurement of relative fluorescence quantum yields. Although the determination of ϕ_f^S appears to be relatively simple, it requires a judicious choice of ϕ_f reference and measurement conditions, and it is prone to numerous artifacts that will be discussed in detail in the next sections of the tutorial.

3 Measuring Fluorescence Spectra

The determination of ϕ_f^S relative to a known standard according to Eq. 7 requires the measurement of the complete fluorescence spectrum of the unknown sample and the reference under conditions that ensure that the same fraction of the emitted photons are detected at all times. Specifically, this fraction should not depend on emission wavelength, and should be the same for the two measurements (i.e. sample and reference). Operating a conventional spectrofluorimeter is surely simple from the technical point of view, but measuring fluorescence spectra under these strict conditions is not. There are sample-related and instrument-related factors that can contribute to the measurement of distorted spectra (that is, the fraction of the emitted photons that are detected by the instrument varies depending on λ_{Em}). Similarly, sample-related and/or instrument-related factors can result in different fractions of photons detected during the acquisition of the sample and the reference emission spectra. While some artifacts can be prevented by carefully choosing reagents and experimental conditions, some are inherent to the instrument and need to be corrected for during or after the measurement.

3.1 Instrumental Factors

There are several instrumental factors that can result in distortions of the measured spectra. For instance, spectral shifts can occur if monochromators are not properly calibrated, and distortions can occur if the detection system does not operate within its linear range. These can be easily prevented by taking basic precautions, as described below. The most important

source of instrument-related spectral distortions is the dependence of the detection system responsivity on emission wavelength. The diffraction gratings used in the monochromators of most instruments have a transmission efficiency that depends on wavelength, and therefore, the fraction of the collected photons that reaches the detector depends on wavelength. Additionally, the photomultiplier tubes (PMTs) used as detectors have a wavelength-dependent response. In general, PMTs are more efficient around 450 nm, and lose efficiency towards the red, resulting in additional distortions of the measured spectra (see Fig. 2). The overall wavelength-dependent efficiency of the detection system is given by these two factors combined, and needs to be taken into account when reporting fluorescence spectra. While reporting technical (uncorrected) spectra may be acceptable in some cases, using corrected spectra is important for the calculation of fluorescence quantum yields.

3.1.1 Excitation and Emission Correction Curves

Measured emission spectra need to be corrected for the wavelength-dependent efficiency of the detection system. The correction is given by a function termed the spectral responsivity function, $s(\lambda_{Em})$:

$$I_f(\lambda_{Em}) = \frac{I_f^u(\lambda_{Em})}{s(\lambda_{Em})} \tag{8}$$

where $I_f^u(\lambda_{Em})$ and $I_f(\lambda_{Em})$ are the uncorrected and corrected spectra, respectively. The uncorrected spectrum is the measured fluorescence spectrum after subtracting background signals (e.g scattering and fluorescence from solvent, see 3.2). The corrected spectrum is instrument-independent and should be always used to calculate fluorescence quantum yields (Eq. 7) and to report fluorescence spectra. The only meaningful information in the spectral responsivity function is the relative values at different wavelengths, and not the numbers in absolute terms. Fig. 2B shows examples of uncorrected and corrected spectra.

Spectral responsitivity functions are usually provided by the instrument manufacturer as emission correction curves, defined as $1/s(\lambda_{Em})$. Photomultiplier tubes are usually most sensitive around 450 nm, so $s(\lambda_{Em})$ as defined in Eq. 8 peaks at that wavelength and decreases towards the red region of the spectrum. Emission correction curves, on the other hand, have a minimum around 450 nm and increase towards the red (Fig. 2A). These curves are usually stored within the software for automated use, and spectral correction is usually given as an option during instrument operation. Researchers should pay attention to whether they are measuring uncorrected, corrected spectra, or both. This type of correction does not need to be performed in real time, and can be carried out after the measurement using Eq. 8 if the function $s(\lambda_{Em})$ is available. Readers should note that spectral correction curves depend on the setting of the emission polarizer when polarizers are used in the measurement. This is because the transmission properties of monochromator gratings depend on polarization, as discussed in section 3.2.3. Therefore, correction curves should be determined for all typical measurement conditions, i.e. without the polarizer, and with the polarizer set in the vertical, horizontal, and magic angle positions (see 3.2.3). See ref. [25] for examples of correction curves for different polarizer settings.

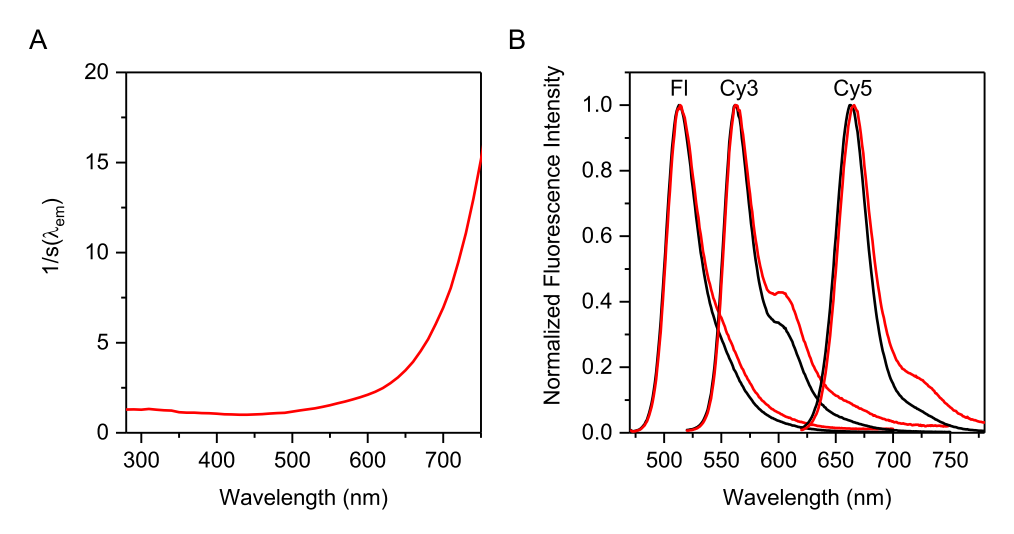


Figure 2: AEmission correction curve for a PTI Quantamaster 4/2005SE instrument equipped with a Hamamatsu R928 PMT. B Uncorrected (black) and corrected (red) spectra for dilute solutions of fluorescein (Fl, in 0.1 M NaOH), Cy3 (in EtOH) and Cy5 (in EtOH).

The most common method for measuring the emission correction curve is to use a calibrated light source placed at the sample position and to compare the measured emission with the certified data for the actual lamp spectral output. This requires a high level of expertise and should be preferably done by specialized technicians. Most companies that commercialize spectrofluorimeters can perform this type of calibration as an optional on-site service. Alternatively, the correction curve can be determined by acquiring the spectra of standard compounds for which the corrected emission spectra are known. Corrected emission spectra for several compounds are available in Appendix 1 of Ref. [8], and a kit certified by BAM (Bundesanstalt für Materialforschung und -prüfung, Germany) is currently commercially available and can be used to cover the 300-770 nm spectral range [26].

Readers should be aware that spectral responsivity functions are sometimes given in power units instead of photon units because data for the spectral distribution of tungsten lamps is usually provided in the form of energy units per unit wavelength interval [27]. This can lead to confusion because converting between energy and photon units requires multiplication by λ ($E = hc/\lambda$), so the shape of the spectral responsivity function is different. The correction curves of most modern spectrophotometers are already provided in photonic units, so this particular issue is typically not a concern. A quick test to ensure that the correction curve provided by the manufacturer is in photonic units is to measure the spectrum of a standard substance, and use Eq. 8 to obtain the corrected spectrum. If the spectrum obtained in this way is grossly distorted it may be an indication that the correction curve was provided in energy units and a conversion using Plank's equation is need.

In addition to the correction curves discussed above, spectrofluorimeters are equipped with a reference channel (usually a quantum counter or a photodiode) that monitors the lamp's output in real time during the measurement. This is used to monitor possible fluctuations in the intensity of the lamp, and more importantly, to correct for wavelength-dependent

variations in I_0 . This is critical for the acquisition of excitation spectra, but unimportant in the determination of relative quantum yields provided that both the sample and reference are excited at the same wavelength. Researchers should note that both types of corrections (excitation and emission) are often available as options within the software, and may not be selected by default.Researchers should also be aware that built-in (i.e. vendor-provided) emission correction curves may not span the whole wavelength range accessible by the instrument.

3.1.2 Detection System Linearity

Most spectrofluorimeters are equipped with photo multiplier tubes (PMTs), which are known to be nonlinear at high intensities of incident light. Instrument manufacturers often recommend maximum intensities to ensure that measurements are within the linear range of the instrument, and measuring within this range is critical to ensure that the intensity measured by the instrument is proportional to the fluorescence intensity emitted by the sample. The most straightforward method to determine the linear intensity range of the detection system of a given instrument is to prepare a series of solutions by serial dilution and to verify that the measured intensity is proportional to concentration. It is important to use solutions with low absorbance (A < 0.04) to avoid deviations due to inner filter effects (see 3.2.2), or otherwise, measured intensities will not be linear even if the system is operating within the detection linear range.

3.1.3 Wavelength Accuracy

In general, there is no need to re-validate wavelength accuracy in commercial instruments unless users suspect problems with the calibration of the monochromators. The most obvious manifestation of a potential problem with wavelength accuracy is a systematic shift in the acquired excitation and/or emission corrected spectra. The corrected emission spectra of several fluorescent standards can be found in Appendix 1 of Ref. [8], and these can be used to assess the wavelength accuracy of the instrument if needed. Because the fluorescence spectra of molecular species in solution are rather wide, a more precise method for the assessment of wavelength accuracy is to use the peak positions of the atomic lines of low pressure atomic lamps (often called pen lamps) [28]. These pens are inexpensive and readily available from vendors that specialize in light sources for research applications.

The position of the Raman peak can be also used to assess the accuracy of one monochromator with respect to the other [28]. The water Raman peak appears at a fixed position with respect to the wavelength of the excitation beam (see section 3.2.1), so this is an inexpensive and straightforward method to evaluate wavelength accuracy in the UV region of the spectrum (Raman intensities are too weak in the visible). Similarly, the scattering intensity from a dilute scattering solution in a standard cuvette can be used to assess a possible bias between the two wavelength selectors. The position of the scattering peak (Rayleigh scattering, see 3.2.1) should coincide with the wavelength of the exciting beam, and any difference indicates that one or both monochromators require re-calibration.

3.2 Sample Factors

3.2.1 Rayleigh and Raman Scattering

So far, we have assumed that incident photons are either absorbed by the sample or transmitted through the solution. However, a fraction of the incident photons may be scattered, and some of these photons may reach the detector and contribute to the measured signals. Scattering is usually categorized as elastic or inelastic depending on whether the energy of the photon is conserved in the process or not. The elastic interaction of light with particles smaller than the wavelength of light is called Rayleigh scattering, and because energy is conserved, the scattered light is detected at a wavelength that equals the wavelength of the excitation beam (Fig. 3). The Rayleigh peak can therefore be avoided by ensuring that the excitation wavelength is lower than the whole range of emission wavelengths scanned in the experiment. Inelastic scattering, commonly called Raman scattering, can be more problematic because the energy of the scattered photons is lower than the energy of the incident photons, increasing the likelihood that the scattered signal overlaps with the fluorescence spectrum of the sample of interest. In aqueous solutions, the Raman peak is due to the O-H stretching mode of water, which occurs near $3,400 \text{ cm}^{-1}$. As a consequence, the Raman peak appears at wavenumbers $3,400 \text{ cm}^{-1}$ higher than the excitation wavelength [16]. In terms of wavelengths, $1/\lambda_R = 1/\lambda_{Ex} - 3.4 \times 10^{-4} \ nm^{-1}$, where λ_R is the center of the Raman peak. Fig. 3 shows the Raman peak of water at three different excitation wavelengths. For $\lambda_{Ex} = 280 \ nm$, a wavelength commonly used to excite tryptophan residues in proteins, the Raman peak occurs at 310 nm and overlaps with the intrinsic fluorescence of the amino acid. It is important to keep in mind that the position of the fluorescence spectrum does not depend on excitation wavelength because, with very few exceptions, the fluorescence transition originates from the lowest vibrational state of the first electronic excited state regardless of λ_{Ex} . In contrast, the position of the Raman peak depends on λ_{Ex} , and this property can therefore be used to distinguish scattering from true fluorescence. Fig. 3, for example, shows that the position of the fluorescence band centered at 350 nm (due to tryptophan fluorescence) is invariant with excitation wavelength, while the position of the Rayleigh and Raman peaks change with excitation wavelength as predicted. Excitation at $\lambda_{Ex} < 270 \ nm$ reduces the contributions of the Raman peak to the measured spectrum, but unfortunately excitation at 290 nm is often preferred in protein research to minimize the contributions of tyrosine residues [8]. Therefore, the Raman peak may be unavoidable, and should be dealt with by examining blank samples and subtracting the scattering contributions from the measured fluorescence spectra.

The Raman scattering intensity is proportional to λ^{-4} , so it is significantly higher in the UV than in the visible. In general, scattering is not a concern for measurements in the visible unless samples are very dilute or quantum yields are particularly low. In the UV, however, scattering intensities are much higher, and the fluorescence signals are generally weaker due to the smaller extinction coefficients that are typical of fluorophores that emit at lower wavelengths. Control experiments run with blank samples (Fig. 3) are always recommended to assess the potential contributions of scattering to the measured fluorescence signals.

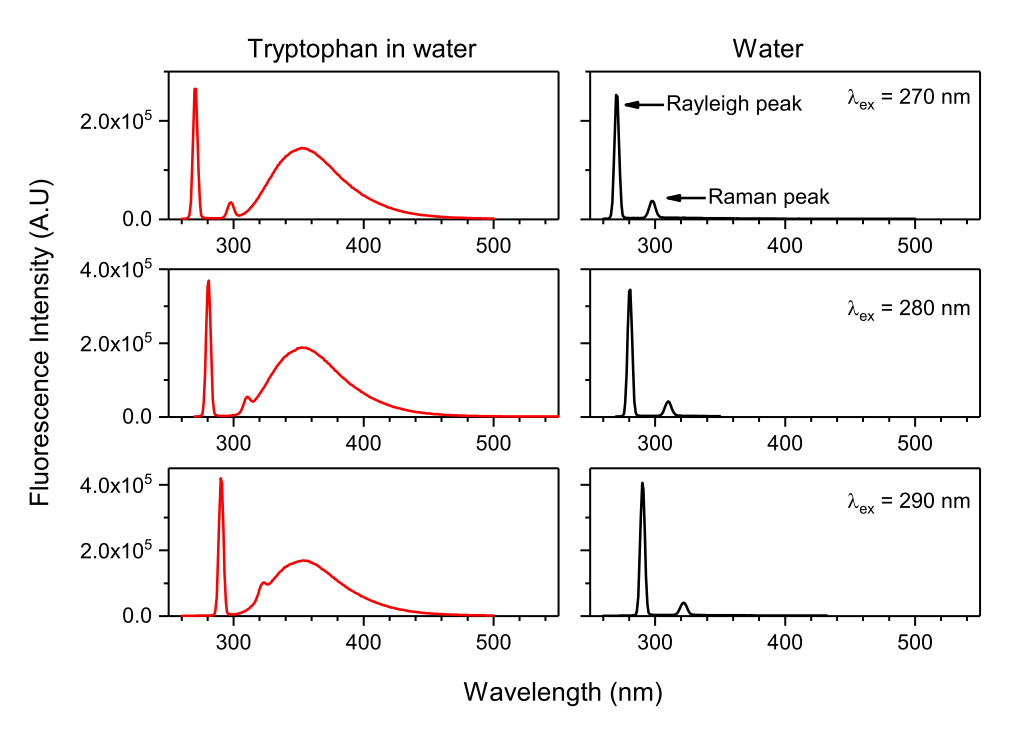


Figure 3: Uncorrected emission spectra of a c.a. $1\mu M$ solution of Tryptophan in water showing the Rayleigh and Raman peaks. Excitation wavelengths were 270 nm (top), 280 nm (middle) and 290 nm (bottom). The signals measured with pure water in the cuvette under identical conditions are shown on the right

3.2.2 Inner Filter Effects

The absorbance of a solution defines a relationship between the intensity of the incident light (I_0) and the intensity of the transmitted light (I_T) , and is proportional to the sample concentration (C), the extinction coefficient (ϵ) , and the path length (b):

$$A(\lambda) = -log(I_T(\lambda)/I_0(\lambda)) = b.\epsilon(\lambda).C$$
(9)

Consider a $1 cm \times 1 cm$ cuvette in an instrument with the traditional right-angle geometry. The detection channel of the instrument is focused at the center of the cuvette, so most photons collected by the instrument are emitted by molecules close to the central part of the cuvette. We can picture the solution as being composed of layers or slabs (Fig. 4). If I_0 denotes the incident excitation intensity for the layer that faces the lamp, then the incident intensity for the layer in the middle of the cuvette (0.5 cm) is the transmitted intensity from the previous layer, equal to $I_0 10^{-0.5 \cdot \epsilon \cdot C} = I_0 10^{-A/2}$ where A is the absorbance of the solution measured with the 1 cm path length cuvette (Eq. 9). If the absorbance of the solution at the excitation wavelength is 0.5, the central part of the cuvette would be excited with an intensity of approximately $10^{-0.25}I_0 \approx 0.56I_0$. The intensity of fluorescence is proportional to the intensity of the exciting beam, and the instrument collects photons emitted from the central part of the cuvette. Therefore, the quantum yield measured in these conditions would be only about 56 % of the value measured for a very dilute solution.

This phenomenon is known as the excitation (or primary) inner filter effect [9,29], and its impact in ϕ_f determinations can be minimized by using dilute solutions $(A(\lambda_{Ex}) < 0.04)$.

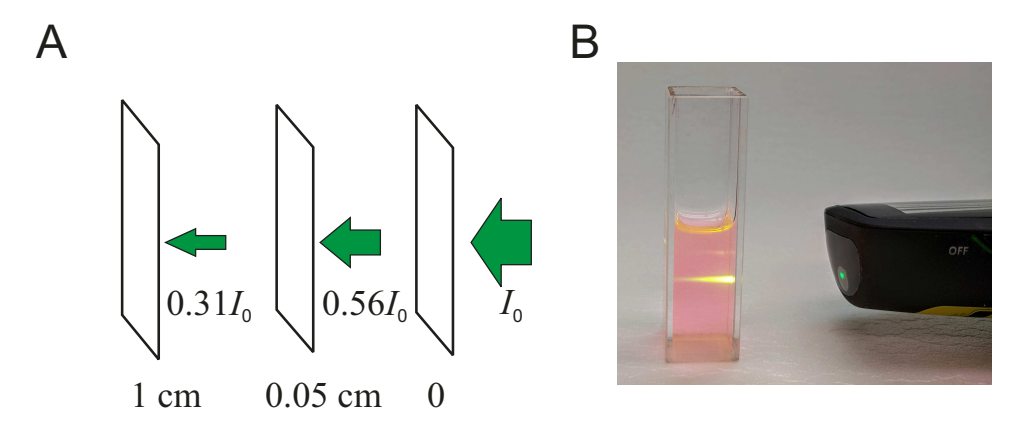


Figure 4: A Schematic representation of a solution in terms of slabs or layers. The solution is excited from the right with intensity I_0 . The incident excitation intensity for each layer is $I_010^{-l.\epsilon.C}$, where l is in centimeters, ϵ is the extinction coefficient in $cm^{-1}M^{-1}$, and C is the molar concentration. The values given in this figure correspond to a solution with A=0.5 at the excitation wavelength (see text). B Photograph of a solution of rhodamine 6G excited with a 532 nm laser pointer. The absorbance of the solution at the excitation wavelength is approximately 2. Fluorescence (yellow) is observed along the path of the laser. Excitation inner filter effects are manifested as a decrease in fluorescence intensity from right to left.

In addition to the excitation inner filter effect described above, photons emitted by a molecule can be re-absorbed by other molecules before reaching the detector. This effect is known as the emission (or secondary) inner filter effect [9,29], and results in both a decrease in the total number of photons emitted by the solution, and a distortion of the spectrum. Consider the absorption and emission spectra of rhodamine 6G in ethanol, shown in Fig. 5. The emission spectrum shown in black was obtained with a solution with $A \approx 0.025$ at the excitation wavelength, where inner filter effects can be considered negligible. The emission spectrum shown in red was measured with a solution about 40 times more concentrated $(A \approx 1)$ at the excitation wavelength). What is the origin of the apparent shift in the emission maximum? In the dilute solution, it is unlikely that a fluorescence photon encounters another molecule before reaching the detector, and therefore the probability that the photon is reabsorbed by another molecule in the solution is low. For the concentrated solution, an emitted photon is likely to encounter another molecule before it reaches the detector. If that photon is re-absorbed, the newly formed excited state may deactivate by a mechanism different from fluorescence, and as a consequence the first emission event will not result in a photon reaching the detector. Importantly, not all photons that collide with other molecules are equally likely to be re-absorbed. Photons emitted on the blue side of the fluorescence spectrum are more likely to be re-absorbed than photons of lower energy (red side) because the former carry energies that match the absorption spectrum of the substance (see Fig. 5, blue curve). Indeed, the shape of the fluorescence spectrum of the concentrated solution matches the spectrum of the dilute solution at wavelengths higher than 575 nm, where the extinction coefficient of this dye is very small. At these emission wavelengths, emitted photons may encounter other molecules, but the probability of re-absorption is very small. The largest discrepancy between the two emission spectra is found at wavelengths where rhodamine 6G absorbs efficiently, as seen in Fig. 5. These distortions give rise to an apparent spectral shift to the red, as shown in the inset of Fig. 5. The effect of self-absorption on the measured spectrum depends on the absorbance of the sample at the wavelengths of the emitted photons. Therefore, it will be more notorious for dyes with small Stokes shifts (large overlap of absorption and emission spectra).

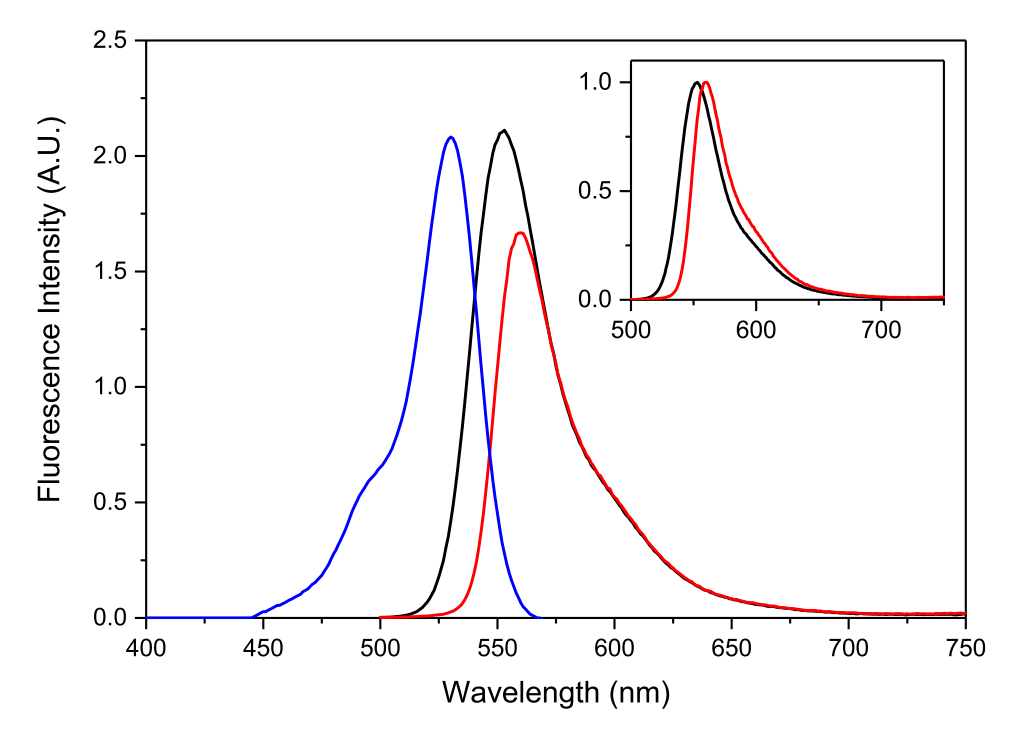


Figure 5: Absorption (blue curve) and corrected fluorescence spectra of Rhodamine 6G in ethanol. The absorption spectrum was scaled arbitrarily. The emission spectra shown in black and red were measured with solutions with an absorbance $A \approx 0.025$ and $A \approx 1$ at the excitation wavelength (495 nm), respectively. The spectra are shown in arbitrary units, and were multiplied by arbitrary constants to match at the red side of the spectrum. Inset: Emission spectra of the same solutions normalized to a peak maximum of 1.

3.2.3 Polarization Effects

Let us reiterate that the use of Eq. 7 requires that the measurements of the fluorescence spectra of the unknown sample and the reference are performed under conditions that ensure that the same fraction of the emitted photons are detected at all times. We have already discussed the instrumental factors that result in wavelength-dependent variations in the transmission and detection of the emitted photons, and how to correct for them. Here, we will discuss polarization effects, which in general lead to the measurement of an intensity that is not truly proportional to the total fluorescence intensity emitted by the sample. An important conclusion of this discussion is that polarization artifacts are important even when no polarizers are used in the experiment, and that the use of polarizers in particular orientations is needed to avoid polarization artifacts in quantitative fluorescence measurements.

One common approach to eliminate polarization effects is to place a polarizer in the vertical position in the excitation path, and a polarizer set at the magic angle (54.7°) in the emission path. The reasons behind this requirement are examined below in detail.

Polarization is a property of light that refers to the direction of the oscillating electric field. In the case of linearly polarized light, the electric field oscillates in a single direction perpendicular to the direction of light propagation. The lamps used in most fluorimeters emit natural (unpolarized) light, which is characterized by a random direction of the electric field. Physically, unpolarized light can be described as a mixture of two independent light streams with equal intensity but perpendicular polarizations (Fig. 6). To understand polarization effects, let us first discuss what happens when we excite the solution with linearly polarized light. To do this, one must use a polarizer to isolate one particular direction of the oscillating electric vector of the exciting light, as shown in Fig. 6. In solution, molecules are expected to be oriented randomly, but only those properly oriented relative to the electric vector of the polarized excitation light can absorb a photon. Readers may be familiar with the concept of transition dipole moment for an electronic transition, which is a quantity related to the extinction coefficient that determines the probability that the molecule will absorb light. However, while the extinction coefficient is a scalar quantity (a number), the transition dipole moment is an oscillating vector that has a defined direction on the nuclear framework of the molecule [8, 9, 17]. For the dye Cy3, for example, the transition dipole moment for absorption in the visible lies along the long axis of the molecule as shown in Fig. 6 [30]. The probability that a molecule will absorb a photon is proportional to $\cos^2\theta$, where θ is the angle between the incident electric field and the absorption transition dipole moment of the molecule (see Fig.S2). This means that molecules with absorption transition dipole moments aligned parallel to the electric vector of the incident light (molecule B in Fig. 6) have the highest probability of absorption, whereas molecules with absorption transition dipole moments aligned perpendicular to the electric vector of incident light (molecule A in Fig. 6) do not absorb at all. Molecule C in Fig. 6 will have a lower probability of absorption than molecule B, and will therefore contribute less to the total number of emitted photons.

Let us assume for a moment that molecules re-orient slowly so that emission occurs from the same orientation the molecule had when the photon was absorbed. For a single molecule, fluorescence emission is polarized along the transition dipole moment that corresponds to fluorescence emission. For Cy3, the emission transition dipole moment is almost parallel to the absorption dipole moment [30], so we can assume that emission is polarized along the long axis of this molecule. Consider now a solution of Cy3 in a highly viscous solvent that prevents molecular rotation during the lifetime of the excited state. Because molecules in certain orientations are more likely to absorb light, the overall fluorescence emission will be partially polarized even if the molecules themselves are randomly distributed in the solution. The polarization of the fluorescence emission can be analyzed in terms of three orthogonal components $(I_z, I_y, I_x, \text{ Figure 6})$. If the excitation polarizer is set in the vertical position as shown in Fig. 6, molecules with orientations close to this axis (e.g. molecule B) are more likely to absorb, and emission will be preferentially polarized along the vertical axis as well (that is, I_z will be larger than I_x and I_y). Fluorescence will not be perfectly polarized

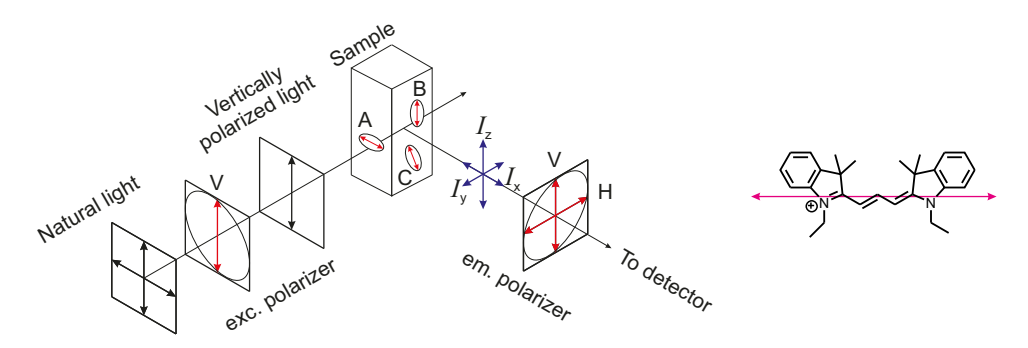


Figure 6: Left: Schematics of a fluorescence measurement using polarizers in the excitation and emission paths. The polarizer in the excitation path (left side of the cuvette) is used to select vertically-polarized light from the natural light emitted by the lamp. The polarization of the fluorescence emission is analyzed in terms of three orthogonal components (I_z, I_y, I_x) . I_z and I_y are measured when the emission polarizer (right side of the figure) is placed in the vertical or horizontal positions, respectively. I_x cannot be measured. Right: A Cy3 molecule. The arrow on the molecule represents the orientation of the transition dipole moment for absorption in the visible band (see text). The probability of absorption is proportional to $\cos^2\theta$, where θ is the angle between the line defined by the transition dipole moment and the electric field of the incident light

along the vertical axis because molecules with other orientations, such as molecule C, still absorb light (although with a lower probability). If molecule C does not re-orient during its excited state, it will emit from an orientation that will lead to $I_y \approx I_z$ because it is at an approximately 45° angle with respect to the vertical axis.

The intensities along the z and y directions can be measured by placing a polarizer in the emission path in the vertical or horizontal position, respectively (Fig. 6). Critical for this discussion, the component along the direction of propagation of the emitted light (I_x) cannot be detected, and this in fact is the key to understand the origin of polarization artifacts when no polarizers are used. We will first consider the intensities measured when the excitation and emission polarizers are placed in vertical (V) or horizontal (H) positions. The measured intensities will be denoted I_{VV} , I_{VH} , I_{HV} , I_{HH} , where the first and second subscripts indicate the orientations of the excitation and emission polarizer, respectively. For the example above (vertical excitation, no re-orientation), we concluded that $I_{VV} > I_{VH}$.

The degree of polarization of the emitted light is usually analyzed in terms of a quantity known as fluorescence anisotropy, defined as

$$r = \frac{I_{VV} - I_{VH}}{I_{VV} + 2I_{VH}} \tag{10}$$

In practice, a correction known as the G-factor is needed because monochromator gratings do not transmit vertically and horizontally polarized light with the same efficiency (see Supplemental Information, Section S3.2). In the case of fluorophores with emission transition dipole moments that lie in the same direction as the absorption transition dipole moments, the measured fluorescence anisotropy is expected to be r = 0.4 if molecules do not re-orient during the lifetime of the excited state [8,9,16]. This value is positive because fluorescence mostly arises from molecules oriented parallel to the excitation light, which is vertically polarized. However, r is lower than 1 because molecules such as molecule C in Fig. 6 still

contribute to the fluorescence signal, and emit light that is not perfectly aligned with the vertical axis of the emission polarizer (i.e. I_y is not zero).

In general, unless the fluorophore is embedded in a a rigid matrix such as a solid or a glass, or measurements are performed at very low temperatures, molecules will re-orient in timescales comparable to the lifetime of the excited state. Rotational diffusion during the lifetime of the excited state results in a partial depolarization of the emitted light [8,9]. For instance, consider molecule B in Fig. 6, which absorbs with the highest probability due to its initial orientation. If the molecule rotates while in the excited state, fluorescence will be emitted from other orientations, decreasing I_{VV} and increasing I_{VH} . In terms of Eq. 10, it is evident that rotational diffusion results in a reduction of r. For example, the fluorescence anisotropy values of aqueous solutions of the dyes Cy3 and Cy3B at room temperature are r = 0.25 and r = 0.045, respectively [31]. The difference is due to the significantly different fluorescence lifetimes of the two dyes ($\tau^{Cy3} = 0.18 \ ns$ and $\tau^{Cy3B} = 2.7 \ ns$) [31]. The value measured for Cy3B, which is close to zero, indicates that rotational diffusion is much faster than fluorescence emission, so that molecules emit from all orientations with almost the same probability, and $I_{VV} \approx I_{VH}$. For Cy3, the almost identical rotational diffusion time results in only a partial depolarization of the emitted light due to the much shorter fluorescence lifetime.

How is this discussion relevant to the measurement of ϕ_f ? In general, the total intensity is $I_T = I_x + I_y + I_z$, but except for specific configurations of the polarizers, the measured intensity is a fraction of this value that depends on the degree of polarization of the emitted light (quantified by r). To start, imagine that you are interested in measuring the fluorescence quantum yield of Cy3 relative to Cy3B. Suppose for the moment that you perform the measurements with polarizers placed in the vertical position in both the excitation and emission channels. For vertically polarized excitation, the z-axis is an axis of symmetry and $I_y = I_x$ (see section S3.1, Supplemental Information file). With this in mind, the total intensity can be expressed in terms of the two measured components $(I_{VV} = I_z, I_{VH} = I_y)$ as $I_T = I_{VV} + 2I_{VH}$. Algebraic manipulation of Eq. 10 gives, $I_{VV} = (2r+1)/3 \times I_T$, and therefore, for this configuration of polarizers, the measured intensity (I_{VV}) would be only a fraction of the total intensity. This on its own is not problem, except that this fraction depends on the degree of polarization of the emitted light, which is different for the sample and the reference. For the Cy3 solution (r = 0.25), $I_{VV} \approx 0.5I_T$, and for the Cy3B solution $(r = 0.045), I_{VV} \approx 0.36I_T$. Therefore, in this case, a higher fraction of the total photons emitted would be measured for the sample (Cy3) than for the reference (Cy3B), resulting in a calculated ϕ_f^{Cy3} about 1.4 times greater than the actual value.

One can naively think that this bias disappears if the emission polarizer is omitted from the measurement, but one must remember that I_x cannot be detected, so the measured intensity would be $I_m = I_z + I_y = I_{VV} + I_{VH}$, which is still a fraction of I_T that depends on r. Algebraic manipulation of Eq. 10 gives, $I_{VH} = (1-r)/3 \times I_T$, so $I_m/I_T = I_{VV}/I_T + I_{VH}/I_T = (2+r)/3$ (see Supplemental Information, Section S3.1). If fluorescence is completely depolarized (r=0), $I_z = I_y = I_x$ and $I_m/I_T = 2/3$ consistent with the fact that one of the three identical components is not detected. If $r \neq 0$, the fraction of the total intensity that is

measured depends on the value of r.

At this point it may seem that the solution is to remove both the excitation and the emission polarizers. In this case, the measured intensity is still $I_z + I_y$ because I_x cannot be detected, and as shown in the Supplemental Information file (section S3.1), $I_m/I_T = (I_z + I_y)/(I_z + I_y + I_x) = (4 - r)/6$, which still depends on the value of r. However, because $0 \le r \le 0.4$, polarization effects are in principle expected to be rather small. Yet, the situation is further complicated by the fact that monochromator gratings do not transmit vertically and horizontally polarized light with equal efficiency. Therefore, even without polarizers, the sample is excited with partially polarized light and detected with a polarization bias, and artifacts can indeed be significance (see section 5.5.5).

How can polarizers help remove polarization artifacts? It can be shown that the use of polarizers in certain orientations allow the detection of a signal that is still a fraction of I_T , but importantly, this fraction is independent of r. The most common approach to achieve this goal is to place the excitation polarizer in the vertical position and the emission polarizer at the so-called magic angle ($\phi \approx 54.7^{\circ}$), defined as $\cos^2 \phi = 1/3$. Readers interested in a derivation for the magic angle conditions are encouraged to read refs. [8,9]. Some instruments have only basic settings for the polarizers, and researchers may find that they can only select the vertical and horizontal position, but not the needed 54.7°. In this case, the total fluorescence intensity can be calculated from the measured I_{VV} and I_{VH} intensities as $I_T = I_{VV} + 2I_{VH}$. However, this requires a correction for the polarization-dependent sensitivity of the detection system (known as the G-factor). For details, see the Supplementary Information File, section S3.2.

4 Measuring Relative Fluorescence Quantum Yields

4.1 Fluorescence Quantum Yield Standards

The precision with which the fluorescence quantum yield of the unknown sample can be determined using Eq. 7 ultimately depends on the accuracy of the value of ϕ_f^R used in the calculation. Values of ϕ_f found in the literature can be surprisingly different even for common compounds that have been widely investigated for decades. For example, literature values of ϕ_f for quinine bisulfate in H_2SO_4 vary from 0.508 to 0.65 [32]. In general, variations may be due to instrumental factors (e.g. inaccurate spectral corrections, see 3.1.1), purity of dyes and solvent, inner filter artifacts (3.2.2), polarization artifacts (3.2.3), or variations in temperature, pH, ionic strength, etc. Researchers should be therefore wary of the many individual measurements published in the literature, and instead rely on values compiled in authoritative sources such the publications and reports from IUPAC (International Union of Pure and Applied Chemistry, USA), BAM (Bundesanstalt für Materialforschung undprüfung, Germany), or NIST (National Institute of Standards and Technology, USA) [12, 14, 33]. The compounds recommended in these publications have been chosen as standards because their fluorescence quantum yields have been investigated systematically with respect to variables such as temperature, excitation wavelength, chromophore concentration, etc.

Importantly, publications from these reputable sources often contain information about the uncertainty of the recommended ϕ_f which reflects the spread of all reliable published values by individual researchers. Examples of recommended standards are shown in Fig. 7 (see Fig. S4 for structures and more information), and readers are encouraged to consult references [12,14,33] for a more comprehensive list of ϕ_f standards. According to an IUPAC report [14], quinine sulfate in H_2SO_4 is the most popular standard for ϕ_f determinations, even in cases where the sample emits in a significantly different region of the spectrum. The reader should note that while quinine sulfate is still a recommended standard [12], the recommended solvent is perchloric acid. The ϕ_f of quinine sulfate displays a more pronounced temperature dependence in sulfuric acid than in perchloric acid [34], so the latter is recommended to minimize uncertainties in the measurements.

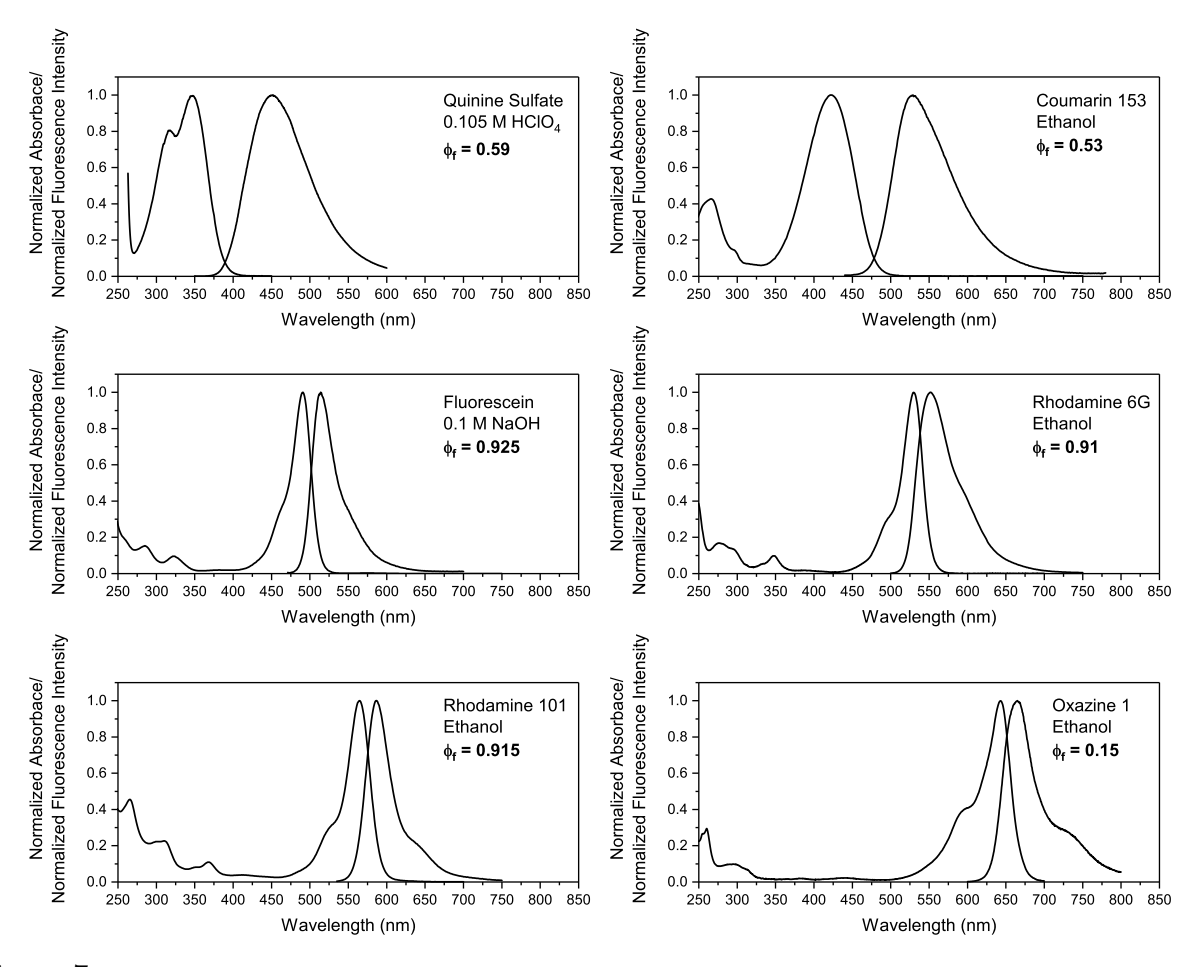


Figure 7: Normalized absorption and corrected emission spectra of some recommended fluorescence quantum yield standards. The structures of the dyes are compiled in the supplemental information file. The ϕ_f values indicated in each case were obtained from reference [12] (except for fluorescein, see refs. [14,35])

One of the main criteria for choosing the reference is that ideally, the standard and sample should absorb and emit in the same spectral regions. Eq. 7 was derived under the assumption that the value of $N_0(\lambda_{Ex})$ in Eq. 5 remains the same during the acquisition of the

sample and the reference emission spectrum. Because the photon flux of the lamp generally depends on wavelength, a correction for the wavelength-dependence of the exciting photon flux would be required if the excitation wavelength used for the sample and for the reference are not the same. This can be done if necessary [13], but should be avoided if possible to minimize the number of factors that contribute to inaccuracies in the measured quantum yield. In addition, as discussed in section 3.1.1, correction curves are needed to obtain the corrected fluorescence spectra from the measured signals. In principle, correction would not be needed if the two solutions (sample and reference) had identical emission spectra. Because this is rarely the case, it is always preferable to use a reference with an emission spectrum similar to that of the unknown sample. This does not eliminate the need for correcting the measured spectra, but minimizes the effects of any inaccuracies that may be introduced during the correction step.

4.2 Experimental Procedures and Considerations

4.2.1 Sample Preparation

High-purity dyes and solvents must always be used to avoid the interference of contaminants. HPLC or spectrophotometric grade solvents are best, but even then, it is always good practice to measure the absorption and fluorescence spectra of the solvent to rule out potential impurities and verify its suitability for the fluorescence experiments. All glassware or plasticware used in sample preparation must be cleaned with care, and samples used for quantum yield determinations must be made fresh if possible. For solutions that have been stored, it is good practice to measure the absorbance spectrum of the solution to rule out possible degradation. For instance, the author has observed a steep decrease in the absorbance in the visible (but not in the UV) of buffered solutions of DNA labeled with the dye Cy5 stored for several months at -20 °C in the dark. While these storing conditions are typical for DNA samples, the Cy5 molecule seems to undergo an irreversible (and certainly unexpected) transformation.

Reference solutions for the determination of relative ϕ_f values are commonly prepared by dissolving the reference dye in a pure solvent. Novice researchers are often tempted to weigh a quantity of the solid to prepare such solutions, but the quantities needed to prepare a few milliliters of a solution with a measurable absorbance (A < 1) are often too small for the sensitivity of common analytical scales. For example, to prepare 2 mL of a solution of tetramethylrhodamine with a peak absorbance of A = 1, one would need to weigh about 8 μg of solid. Knowledge of the concentration is not needed to calculate ϕ_f , so there is no need to measure the mass of dye used in the preparation of the solution. Instead, it is sufficient to grab a very small particle of solid with a needle or a pipette tip, and dissolve it in the desired solvent. If the absorbance of this solution is too high, as is frequently the case, successive dilutions should be made until the desired absorbance is achieved.

4.2.2 Cuvettes

A variety of cuvettes for fluorescence spectroscopy are available from vendors that specialize in laboratory equipment. Cuvettes may differ in optical length, volume, shape and the material of the optical windows. Most cuvettes are made of glass or quartz. Although glass is cheaper, it absorbs strongly in the UV limiting the use of these cuvettes to the range 360-2,500 nm. Quartz cuvettes, on the other hand, can be used down to 200 nm, enabling the measurement of important biological molecules such as tryptophan. Except for specialized cuvettes (e.g. for front-face fluorescence measurements), fluorescence cuvettes generally have an external 1 $cm \times 1$ cm square cross section and at least three optical windows. Two optical windows are on parallel faces of the cuvette and used to measure the transmittance (and therefore the absorbance) of the solution. At least one of the perpendicular faces of the cuvette (and often both) contain optical windows for fluorescence measurements using instruments with a 90° geometry. Depending on the cuvette, the path length along these two directions may be different. For instance, the three cuvettes shown in Fig. 8 have a 1 cm-path length in the direction orthogonal to the plane of the figure, but different path lengths in the perpendicular direction. The cuvette shown in the middle has optical windows in all four faces, and can be used in absorbance measurements in either direction (albeit with different optical path lengths). The cuvette shown on the right has only three optical windows, while the fourth side of the cuvette is not transparent (see Fig. 8D). This cuvette needs to be oriented along the 1 cm-path length direction for absorbance measurements, and the perpendicular window needs to be oriented towards the emission detection channel for fluorescence.

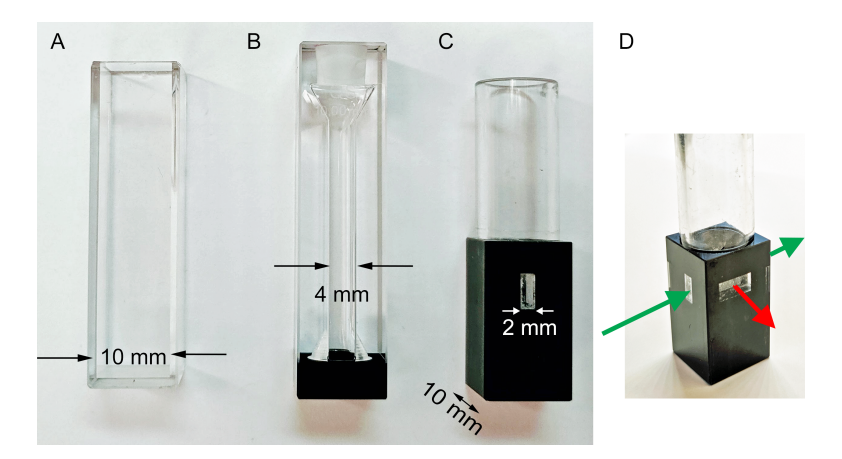


Figure 8: ATraditional fluorescence cuvette with four optical windows and a $10~mm \times 10~mm$ path length. B Semi-micro fluorescence cuvette with a $10~mm \times 4~mm$ path length. The bottom of this cuvette is designed to hold a small stirring bar. C Ultra-micro fluorescence cuvette with a $10~mm \times 2~mm$ path length. This cuvette has three optical windows (the side facing left is opaque). D Same cuvette rotated clockwise. There are two parallel optical windows separated by 1~cm for absorbance measurements (green arrows) and a perpendicular window with a 2~mm path length to measure fluorescence (red arrow)

Most cuvettes do not need to be completely filled, but it is critical that there is enough sample in the cuvette for the incident light to go through the solution and not air. Standard

 $1cm \times 1cm$ cuvettes require about 2 mL of solution, while ultra-micro cuvettes that require as little as 12 μ L can be purchased from vendors such as Hellma. Ultra-micro cuvettes have smaller optical windows, so it is critical that the height of the center of the sample compartment is well aligned with the incident beam. The height of the light beam varies among different manufacturers of spectrophotometers and spectrofluorimeters, so knowledge of this height (usually called the z-dimension) is a pre-requisite to select a cuvette compatible with a specific instrument. Although working with smaller volumes seems like an obvious advantage, the small size of the optical window of these cuvettes makes it challenging to obtain accurate and reproducible measurements of absorbance and fluorescence. If possible, it is always better to use a cuvette with an optical window larger than the size of the beam. This will require larger sample volumes, but will minimize uncertainties in all measurements.

4.2.3 Measuring the Absorbance of the Solution

The calculation of ϕ_f relies on precise knowledge of the absorbance of both the sample and reference solutions. The measurement of the absorbance of a solution is typically performed with a spectrophotometer using the same cuvettes that will be used for the acquisition of the fluorescence spectra. A double-beam spectrophotometer is the best choice to maximize analytical precision, but even then, it is always a good idea to measure the full spectrum of the sample (as opposed to just the absorbance at the desired wavelength) to check for any baseline offsets and for potential contributions of scattering to the baseline. Scattering occurs when light interacts with particles smaller than the wavelength of light such as colloids, aggregates or large protein assemblies. The scattering intensity is proportional to the inverse of the fourth power of the wavelength, resulting in a baseline that increases rapidly with decreasing wavelength. This is illustrated in Fig. 9, which shows the absorption spectra of Sulforhodamine 101 in water together with the spectrum of the same solution containing a small quantity of colloidal silica. Both spectra were measured using water in the reference compartment of the spectrophotometer. Scattering is particularly problematic and difficult to correct for in the UV region of the spectrum, so it should be prevented if at all possible.

The accuracy of absorbance measurements is best in the range A ≈ 0.5 –1, but values lower than c.a. 0.04 are needed to avoid inner filter effects. Whether the small absorbance values needed for the ϕ_f determination can be measured directly with precision depends on the quality of the spectrophotometer. Typically, accuracy is improved by measuring the absorbance of a stock solution with an absorbance in the range A = 0.5–1, and performing a precise dilution to obtain the desired absorbance A < 0.04. This of course relies on the assumption that the absorbance of the solution is linear with concentration in this range. An obvious control is to verify that the shape of the spectrum of the stock solution is identical to the shape of the spectrum of the dilute solution except for noise. For example, xanthene dyes such as fluorescein and rhodamine derivatives form dimeric assemblies in aqueous solution with a plane-to-plane stacking geometry (H-dimers) and a characteristic absorption band that overlaps with the absorption shoulder of the monomer. As a consequence, the dimerization of these dyes results in an apparent increase in the absorbance of the monomer [36,37]. Fig. 10 illustrates this point. The visible spectrum of a $6.6 \times 10^{-6} M$ aqueous solution of

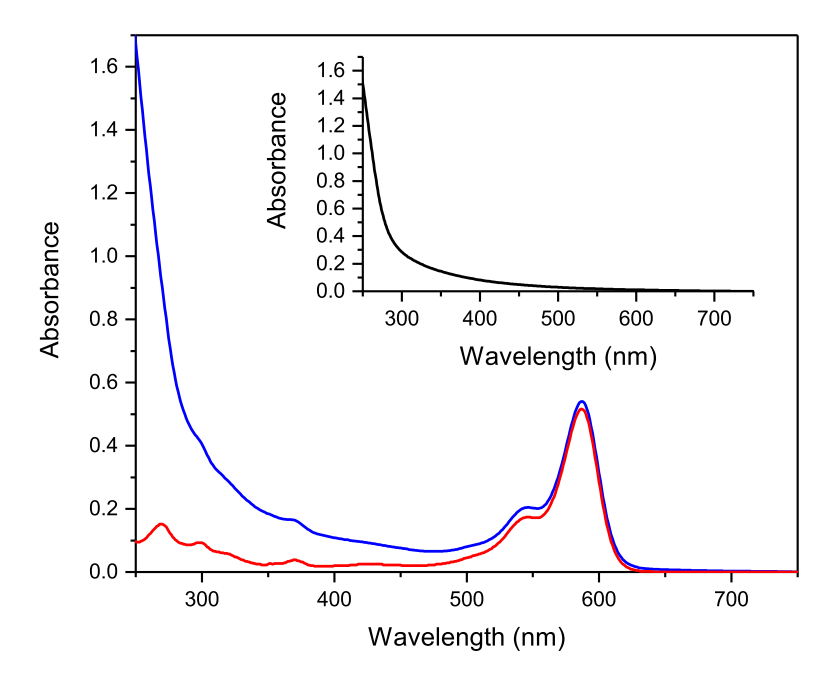
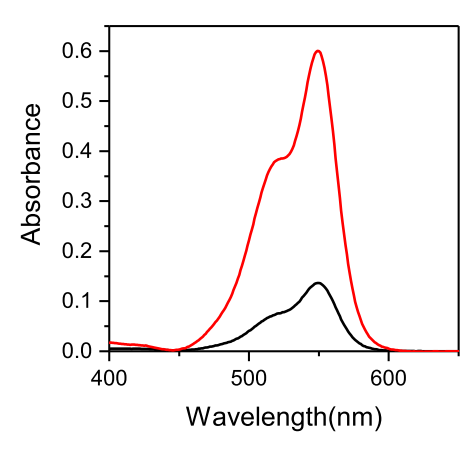


Figure 9: Absorption spectrum of sulforhodamine 101 in water (red) and in water containing a small quantity of Ludox (colloidal silica, blue curve). Water was used in the reference compartment of the spectrophotometer in both cases. Inset: "Absorbance" spectrum of the Ludox solution alone. The signal is not due to absorption, but to the scattering of light by the small colloidal particles (see text).

tetramethylrhodamine has an absorbance of c.a. 0.4 at 520 nm, which would be optimal for an accurate determination. However, a comparison of the normalized spectrum of this solution with the spectrum of a $1.5 \times 10^{-6} M$ solution of the same dye shows the characteristic spectroscopic signature of the dimeric form of rhodamine, i.e., an increase in the absorbance of the shoulder band. The spectrum of the dilute solution coincides with the spectrum of the monomeric form of the dye, but the spectrum of the more concentrated solution shows a clear contribution from the dimer. As a consequence, the absorbance of these solutions is not proportional to the concentration of dye, and the dilution step recommended above would lead to an erroneous estimate of the absorbance of the dilute solution.

4.2.4 Choosing the Excitation Wavelength

The determination of ϕ_f requires integration of the whole fluorescence spectrum of both the sample and the reference solutions. This requires an excitation wavelength that is short enough so that the whole emission spectrum can be scanned without interference from the Rayleigh scattering peak discussed in section 3.2.1. A common mistake is to excite at the absorption maximum of the chromophore, but this often results in the truncation of the fluorescence spectrum on the high-energy (low-wavelength) side (Fig. 11, inset). Another criterion for the selection of the excitation wavelength is the precision with which the absorbance can be determined, which depends on the slope (steepness) of the absorption spectrum at the wavelength of interest. Absorbance measurements are more precise when taken on a plateau



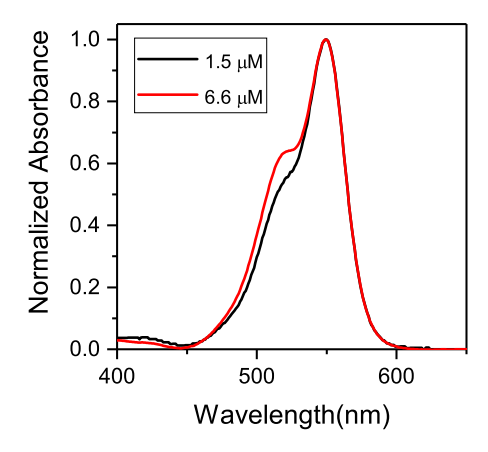


Figure 10: Absorption spectra of $1.5\mu M$ (black) and $6.6\mu M$ (red) tetramethylrhodamine in water. The normalized spectra shows an increase in the absorbance at 520 nm characteristic of the dimer of rhodamine dyes. The spectrum shown in black coincides in shape with the spectrum measured in ethanol, where dimerization is negligible.

than on a sharp slope. Otherwise, small errors in the wavelength accuracy of the instruments and differences in the monochromator bandwidths of the spectrophotometer and the spectrofluorimeter can lead to significant uncertainties in the values of the absorbance. For example, the optimal excitation wavelength for a solution of sulforhodamine 101 in ethanol is the plateau around 535 nm, which allows the determination of the full fluorescence spectrum (Fig. 11, red).

4.2.5 Temperature Control and Measurement

The fluorescence quantum yield of most fluorophores depends on temperature, so controlling and measuring the temperature of the solution is critical to improve the precision of the determination, even at room temperature. Most spectrofluorimeters have cell holders with an inlet and outlet to circulate temperature-controlled water using an external water circulation thermostat. Some instruments have Peltier-based temperature-controlled cuvette holders that allow for temperature control using the instrument's software. Regardless of the method used for controlling temperature, it is recommended that the actual temperature of the solution be measured inside the cuvette. This can be achieved using a digital thermometer equipped with a thermocouple bead wire temperature probe (see Fig. S7).

4.2.6 Influence of Oxygen

Molecular oxygen is a well-known quencher of fluorescence [8,9]. For quenching to be efficient, an oxygen molecule needs to collide with a dye molecule during its excited state (that is, oxygen quenching is a collisional process). The efficiency of this process, therefore, is higher for dyes with long lifetimes, and in conditions in which molecular diffusion is faster (e.g. low solvent viscosity and high temperature). The rate constant for a diffusion-controlled reaction can be calculated from the diffusion coefficients $(D_{A,B})$ and the hydrodynamic radii $(r_{A,B})$

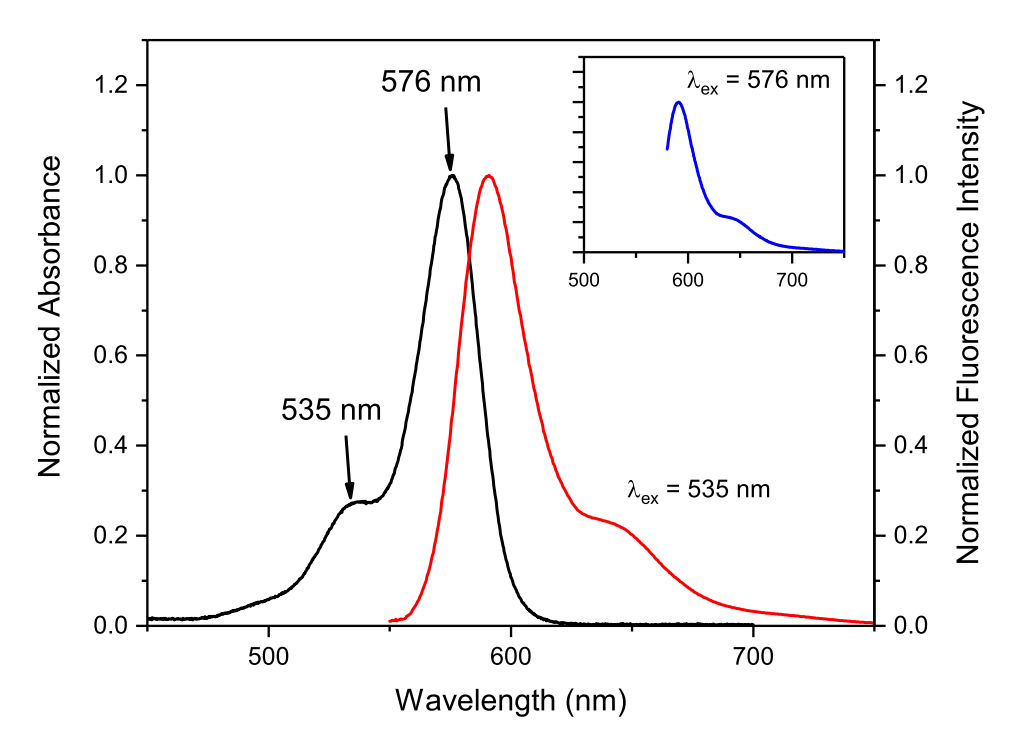


Figure 11: Normalized absorption and emission spectrum of sulforhodamine 101 in ethanol. The curve in red was obtained exciting at 535 nm, which allows the acquisition of the full emission spectrum. Inset: Excitation at the absorption peak (576 nm) forces the researcher to start the emission scan at $\lambda_{Em} > 576nm$, which results in a truncated spectrum.

of the two interacting molecules (in this case, molecular oxygen and the fluorophore), and is of the order of $k = 10^{10} M^{-1} s^{-1}$ for oxygen in water at room temperature. Assuming that quenching is a diffusion-controlled process, as has been demonstrated for aromatic hydrocarbons [38], the product $k[O_2]$ is a pseudo-first order reaction constant for the quenching of fluorescence by oxygen. For water in equilibrium with the atmosphere, the concentration of dissolved oxygen is $2.7 \times 10^{-4} M$, which gives $k[O_2] \approx 3 \times 10^6 s^{-1}$. For quenching to be efficient, this rate needs to be comparable or greater than the rate of fluorescence emission, which is given by the inverse of the fluorophore's lifetime. In other words, the value of $1/k[O_2] \approx 330 \text{ ns}$ needs to be similar or smaller than the lifetime of fluorescence of the dye. Consistent with this, quenching by dissolved oxygen is negligible for most common fluorophores, which have lifetimes of the order of a few nanoseconds, but very efficient for fluorophores such as pyrene, which have lifetimes in the hundreds of nanoseconds [8,9]. If needed, the concentration of oxygen in the solvent can be reduced by bubbling nitrogen or argon gas, or by freeze-pump-thaw cycling. Regardless of the method, degassing can cause concentration changes that need to be accounted for by measuring the absorbance of the degassed solution in a well-sealed cuvette.

4.2.7 Integration of the Corrected Fluorescence Spectrum

The focus so far has been on ensuring that the measured fluorescence spectrum is an accurate representation of the true fluorescence spectrum of the sample. This requires a careful choice of experimental conditions and the use of correction factors. Once this is accomplished, the calculation of ϕ_f according to Eq. 7 requires the integration of the measured corrected fluorescence spectrum. Integration should be performed as a function of wavelength (as opposed to wavenumber) because all instruments are equipped with grating monochromators, and these operate at a constant wavelength bandpass. The limits of integration in 7 indicate that all photons emitted by the sample should be counted regardless of their energy. In practice, however, integration over an infinite wavelength range is neither feasible nor appropriate. The limits of integration should be wide enough to cover the whole spectrum, but also limited to avoid unnecessary contributions of background, scattering, or other spurious contributions to the signal. The software that comes with most instruments usually includes integration tools that can be used to calculate the integral of the measured corrected spectrum. Otherwise, various computer programs such as Origin, Igor Pro or Sigmaplot include similar integration tools. Because fluorescence spectra are usually measured in 0.5 or 1 nm steps, several hundreds of points are collected during the scan and the area under the curve (i.e. the needed integral) can be approximated by adding the values of all the measured intensities and multiplying the result by the size of the wavelength acquisition step used in the experiment (e.g. 0.5 nm). For example, for the fluorescence spectrum shown in Fig. 11, this method results in an estimated area that is only $5 \times 10^{-3}\%$ different from the value obtained by integrating the curve using mathematical software.

5 A step-by-step example

In this section we will walk the reader through an example to illustrate how to implement the information provided in previous sections. All files acquired in the experiments described below are provided as supplementary information. Let us assume that we are interested in determining the fluorescence quantum yield of the dye Cy3 (nonsulfonated, see Fig. S4) in 50% (V/V) glycerol, and for the purpose of this exercise, let us assume there is no spectroscopic data reported in the literature for this compound.

5.1 Preparation of the solution of interest

We are interested in determining the fluorescence quantum yield of Cy3 in 50% glycerol. The 50% (V/V) glycerol solution (solvent) was prepared by mixing equal volumes of doubly distilled water and pure glycerol (Alfa Aesar, spectrophotometric grade). As mentioned in section 4.2.1, just a few micrograms of the solid are needed to prepare the solution, but this mass does not need to be measured or known. Accordingly, to prepare the solution, we just grabbed a barely visible amount of solid with a pipette tip, and dissolved the solid in 2 mL of 50% (V/V) glycerol.

5.2 Initial spectroscopic characterization

We are assuming that no spectroscopic data is available for this compound, so we need to acquire preliminary absorption and emission spectra to be able to choose an appropriate quantum yield reference. We do not need rigorous conditions yet (e.g. magic angle conditions or temperature control), but the absorbance of the solution needs to be kept at a reasonable value to avoid re-absorption effects that can distort spectra severely (see section 3.2.2). Based on our experience, we avoid using small-volume cuvettes unless absolutely necessary, so for this determination we chose standard $1cm \times 1cm$ quartz fluorescence cuvettes (Fig. 8, see (4.2.2). The absorbance spectrum of the sample prepared in 5.1 was acquired using 50% (V/V) glycerol solution in the reference channel of the spectrophotometer (Fig. 12). As discussed in section 4.2.4, spectral shoulders are usually good choices for λ_{Ex} , but the absorbance of this solution is about an order of magnitude higher than the values recommended to minimize inner-filter effects (section 3.2.2). For this reason, we made a dilution to obtain an absorbance of approximately 0.05 at the shoulder of the spectrum, and then measured the emission spectrum of this dilute solution exciting at 514 nm (the shoulder of the absorption spectrum). The measured preliminary emission spectrum is shown in Fig. 12. The goal of this step is just to inspect the spectrum of the unknown sample to have the information needed to choose an appropriate quantum yield standard, so we did not use polarizers, and we did not control the temperature of the cuvette. In this step, it is only important to avoid artifacts that can greatly distort the shape of the spectrum, such as re-absorption (emission inner filter effect) or working above the linear range of the detector (section 3.1.2). Accordingly, the excitation and emission slits were adjusted to ensure that the uncorrected signals were within the linear range of the instrument.

5.3 Choice of fluorescence quantum yield standard

A discussion of the considerations that need to be taken into account for choosing a standard was presented in section 4.1. We inspected the spectral data reported in the references cited in that section (see Fig. 7 for a partial list), and determined that the absorption and emission spectra of the compound rhodamine 6G in ethanol are the closest to the spectra of our sample (Fig. 12). We therefore proceeded to prepare a solution of rhodamine 6G in spectrophotometric grade ethanol following the same procedure reported above for the Cy3 solution. The absorption spectrum of this solution (using ethanol in the reference channel of the spectrophotometer) is shown in Fig.13A.

5.4 Preparation of the sample and reference solutions for the ϕ_f measurements

The solutions prepared initially are too concentrated for a ϕ_f determination. As explained in this tutorial, it is best to keep the absorbance of the solutions lower than c.a. 0.04 at the excitation wavelength to minimize inner filter effects (section 3.2.2), but as shown in Fig. 13A, the absorbance values of both solutions are too high by over an order of magnitude.

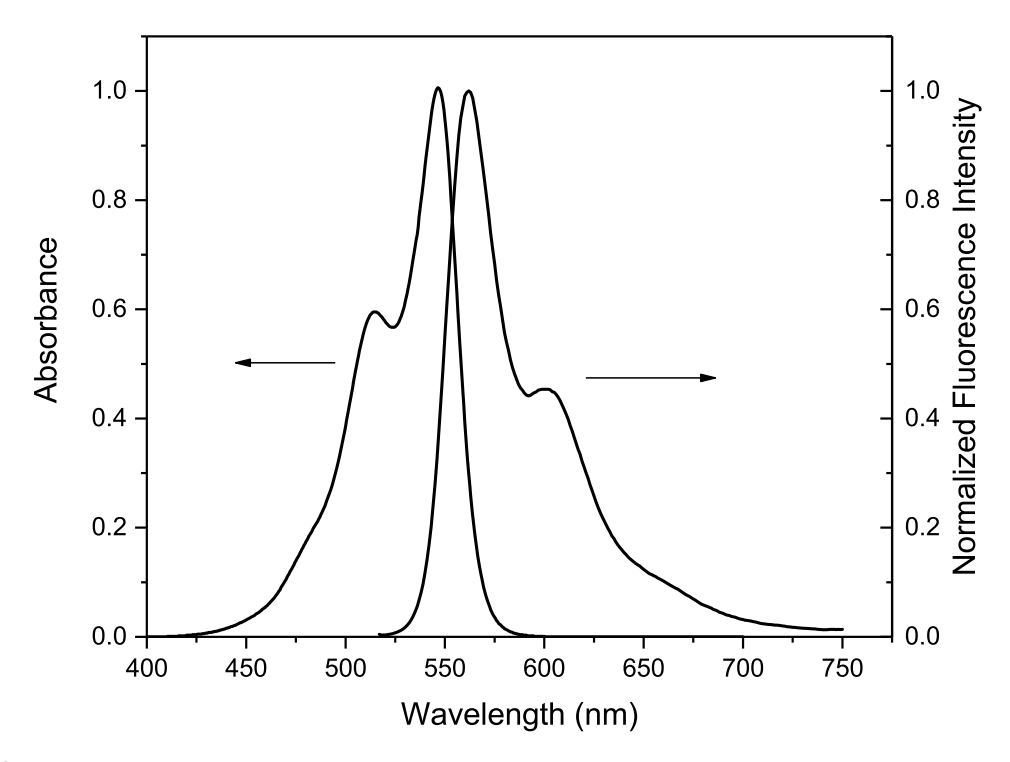


Figure 12: Absorption and preliminary corrected emission spectra of the Cy3 solution prepared in 5.1 (measured in a $1cm \times 1cm$ cuvette). Absorbance values are as measured, while emission intensities were normalized to a maximum value of 1. The solution was diluted 17-fold prior to the acquisition of the emission spectrum to minimize inner filter effects. Excitation wavelength was 514 nm.

We note that the initial spectroscopic characterization described above (see 5.2) just requires that the absorbance is low enough to avoid distortions in the spectrum (i.e. emission inner filter effects), but in this step it is also important to avoid excitation inner filter effects. To achieve the desired low absorbance values, one could dilute the stock solutions and measure the absorbance again, or rely on the dilution factor to re-calculate the new absorbance assuming that absorbance is proportional to concentration in the conditions used in the experiments (section 4.2.3). We have a standard dual-beam UV-VIS spectrophotometer (Shimadzu UV-1700), which is not accurate at the low absorbance values needed for the ϕ_f determinations. For this reason, we prefer to measure more precise values (around $A \approx 0.5$) and perform a precise dilution to obtain the desired absorbance. In this case, we chose to perform a precise 1:25 dilution of the rhodamine solution, and a 1:17 dilution of the Cy3 solution. The second dilution factor was chosen so as to match the absorbances of both solutions as much as possible at the wavelengths used to excite the samples during the acquisition of the emission spectra. The calculated absorption spectra of these dilutions are shown in Fig. 13B.

As mentioned in section 4.2.3, one potential concern is dye aggregation, which would result in spectral changes and a non-linear relationship between absorbance and concentration. For this reason, we performed a quick control experiment to verify that the spectrum of Cy3 in 50% (V/V) glycerol does not change upon dilution, and that absorbance is proportional to

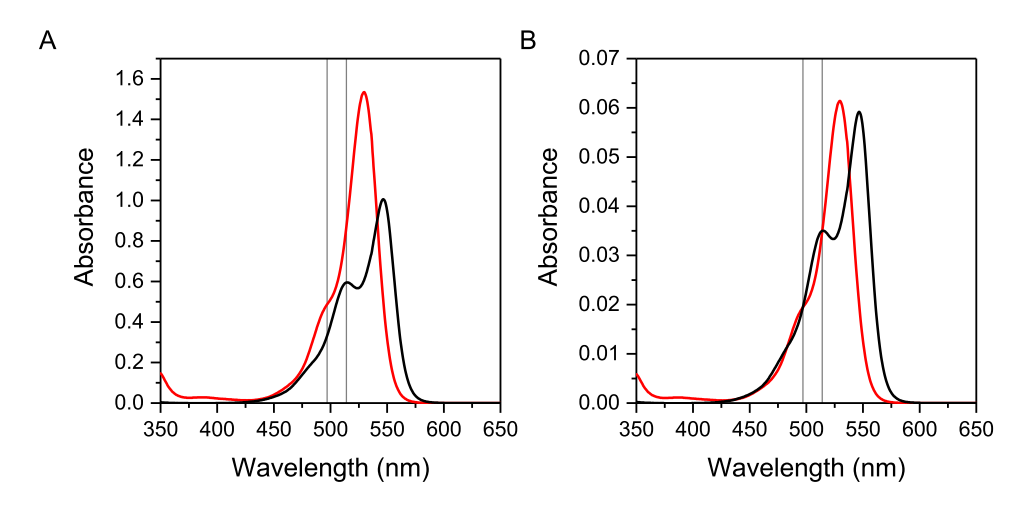


Figure 13: A Absorbance spectra of the rhodamine 6G (ethanol) and Cy3 (50% glycerol) solutions prepared originally as described in 5.1. The vertical lines correspond to the two wavelengths used as excitation wavelength for the acquisition of the fluorescence spectra (497 nm and 514 nm). B Calculated (not measured) spectra of the 1:25 and 1:17 dilutions (rhodamine 6G and Cy3, respectively) described in the text. The grey lines indicate the excitation wavelengths used to acquire the emission spectra

concentration in this range. The results are shown in Fig. S5. We did not perform the same control for rhodamine 6G in ethanol because there is ample information in the literature that rules out dimerization of rhodamines in ethanol at these concentrations [36,37].

5.5 Fluorescence measurements

5.5.1 Excitation wavelength

The criteria to choose the value of λ_{Ex} for the acquisition of the fluorescence emission spectra were discussed in section 4.2.4. The shoulders (or plateau regions) in the absorption spectra are usually good choices, but in this case the optimal excitation wavelength for the sample (514 nm, see Fig. 13) is not a plateau region for the reference. For this reason, we decided to acquire spectra at two different excitation wavelengths that correspond to the spectral shoulders of the standard and reference, 497 nm and 514 nm (indicated with gray lines in Fig. 13). Using more than one excitation wavelength is in fact good practice and always recommended.

5.5.2 Experimental details

Fluorescence emission spectra were acquired using a PTI Quantamaster 4/2005SE spectrofluorimeter (Fig. S7A) using the same solutions and cuvettes used to acquire the absorption spectra shown in Fig. 12B. The absorbance of these solutions is low enough to minimize inner filter effects. All spectra were measured with the excitation polarizer fixed in the vertical position and the emission polarizer fixed at the magic angle to eliminate polarization artifacts (section 3.2.3). The slits of the instrument were adjusted to 2 nm to ensure that the

uncorrected signals (i.e. the signals detected by the instrument) were always lower than the maximum recommended by the manufacturer of our instrument (section 3.1.2). We have independently verified that signals are indeed linear in this recommended range. Temperature was controlled using a water circulation system. The inlet and outlet that connect to the sample holder are shown in Fig. S7B. Temperature was measured inside the cuvette using a digital thermometer with a mm-sized probe (Fig. S7C). In our experience, temperature should be measured inside the cuvette placed in the cuvette holder with the lid of the instrument closed, especially when the thermostat is set at temperatures significantly different from the ambient temperature. For these measurements, we set the thermostat so that the temperature measured inside the cuvette was $25^{\circ}C$.

All signals were corrected during the measurement using the emission correction curve provided by the instrument's manufacturer, which is stored within the software of the instrument. The acquired corrected emission spectra are shown in Fig. 14. We also acquired the spectra of the two solvents (pure ethanol and 50 % glycerol (V/V), see Fig. S6), and determined that these signals were negligible compared to the emission signals of the two fluorescent samples. Otherwise, we would have subtracted the blanks from the measured spectra before applying spectral corrections.

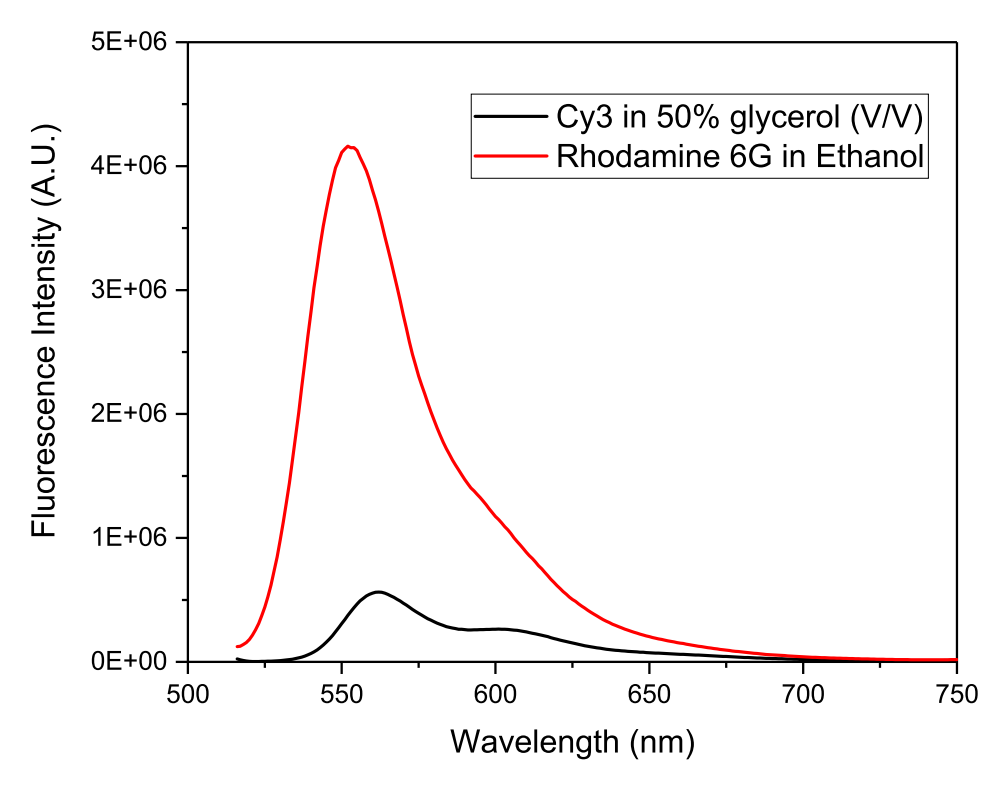


Figure 14: Corrected fluorescence emission spectra of Cy3 (in 50% glycerol, black line) and rhodamine 6G (in ethanol, red line) under magic angle conditions. The solutions are the same as the ones used to acquire the absorption spectra of Fig. 13B. Excitation and emission slits were set at 4 nm. Excitation wavelength was 514 nm. Temperature was controlled and measured inside the cuvette as $25^{\circ}C$.

5.5.3 Calculations

The calculation of ϕ_f^S using Eq. 7 requires integration of the spectra shown in Fig. 14, the values of the two absorbances at the excitation wavelength, literature (or experimental) values of the indices of refraction of the solvents, and an authoritative value of ϕ_f^R .

We integrated the spectra of Fig. 14 using Origin Pro (see section 4.2.7) and obtained $\int_0^\infty I_f^R(514nm, \lambda_{Em})d\lambda_{Em} = 2.223 \times 10^8$ for rhodamine 6G and $\int_0^\infty I_f^S(514nm, \lambda_{Em})d\lambda_{Em} = 3.235 \times 10^7$ for Cy3. The measured absorbances of these samples at 514 nm (Fig. 13B) were 0.0349 and 0.0350 for rhodamine 6G and Cy3, respectively. The refractive indices of 50% (V/V) glycerol (sample) and ethanol (reference) are $n_S = 1.40703$ and $n_R = 1.3611$. Using these values in Eq. 7, we get:

$$\frac{\phi_f^S}{\phi_f^R} = \frac{n_S^2}{n_R^2} \times \frac{\int_0^\infty I_f^S(\lambda_{Ex}, \lambda_{Em}) d\lambda_{Em}}{\int_0^\infty I_f^R(\lambda_{Ex}, \lambda_{Em}) d\lambda_{Em}} \times \frac{(1 - 10^{-A^R(\lambda_{Ex})})}{(1 - 10^{-A^S(\lambda_{Ex})})} = 0.155$$
 (11)

Finally, using $\phi_f^R = 0.91$ [12], we get $\phi_f^S = 0.141$.

The same procedure with the data acquired using $\lambda_{Ex} = 497 \ nm$ gives $\phi_f^S = 0.138$. The percent difference between the ϕ_f^S values obtained at 497 nm and 514 nm is 2.2%. Given the precision of the reported value of $\phi_f^R = 0.91$ and all the uncertainties in the measurements involved in the calculation of ϕ_f^S we would report the fluorescence quantum yield of Cy3 in 50% glycerol (25 °C) as $\phi_f = 0.14$. Readers are encouraged to follow common practices to ensure reproducibility of the results and to estimate the uncertainty of the measurement from the standard deviation of as many repeats as possible.

5.5.4 Are spectral corrections necessary?

We repeated the measurements using $\lambda_{Ex} = 514 \ nm$ under magic angle conditions but we omitted the spectral responsivity corrections in all measurements. The calculated ϕ_f^S under these conditions was 0.117, a value c.a. 17% lower than the value measured when the proper spectral corrections are applied. This is not surprising as the emission of the sample (Cy3) is red-shifted with respect to the emission of the reference, and the sensitivity of the instrument decreases towards the red. Therefore, the Cy3 signals are more underestimated than the rhodamine 6G signals, resulting in a lower ratio of the integrated intensities.

5.5.5 Are polarizers necessary?

We repeated the measurements using $\lambda_{Ex} = 514 \ nm$ but omitting the polarizers in both the excitation and emission channels. The calculated ϕ_f under these conditions was 0.117, a value c.a. 17% lower than the value measured with polarizers. This value is equal to the value obtained when ignoring spectral correction by coincidence. The fluorescence anisotropies of these solutions were measured using Eq. 10 and taking into account the corrections (G-factor) described in the supplemental information section. The measured anisotropies were r = 0.282 and r = 0.019 for the sample and reference, respectively. The relatively high

fluorescence anisotropy value for the Cy3 solution is responsible for the polarization artifacts introduced by not using polarizers during the measurement, as discussed in section 3.2.3.

We also calculated ϕ_f^S using data acquired without polarizers and without taking into account spectral corrections, and obtained $\phi_f^S = 0.098$, a value c.a. 31% lower than the value measured in 5.5.3. This significant discrepancy highlights the importance of being rigorous when using fluorescence as a quantitative tool.

6 Conclusions

The main objective of this tutorial was to provide researchers with the tools needed to avoid common artifacts in fluorescence spectroscopy, and to incentivize investigators to evaluate rigorously the variables that affect the quality of the data they report. Although there are several resources available to investigators with ample experience with fluorescence techniques [13, 15, 28, 39–41], these can be overwhelming to researchers with expertise in other fields that use fluorescence, but do not have a strong background in this field. The experimental acquisition of fluorescence spectra is straightforward from the technical point of view, but as we discussed in this tutorial artifacts are commonplace. One of the most common pitfalls is illustrated in Fig. 4, which shows severe distortions in the measured spectrum due to secondary inner filter effects. Reporting uncorrected spectra spectra is also commonplace, but the impact of this depends greatly on the application. It is critical that researchers are clear on whether they publish corrected or uncorrected spectra so readers can evaluate critically the information that is being reported. For instance, as shown in Fig. 2, the corrected and uncorrected spectra of the common FRET dye Cy3 are noticeable different. This difference is significant in the calculation of the FRET overlap integral, which is one of the factors that determine the value of the Förster distance R_0 . Raman scattering is another common source of artifacts, especially in the UV region of the spectrum.

The determination of fluorescence quantum yields is also conceptually simple but subject to many sources of error. Common pitfalls include not using a suitable ϕ_f standard, measuring in conditions where inner filter effects are significant, and ignoring spectral corrections. As demonstrated in section 5, the use of polarizers in the so-called magic angle conditions is also important when using samples with large values of fluorescence anisotropy. Some researchers wrongly believe that a low fluorescence anisotropy value is guaranteed for organic fluorophores in fluid solution, but this ignores the fact that this is true only for fluorophores with relatively long fluorescence lifetimes. As described in our example, the fluorescence anisotropy of a small dye like Cy3 is relatively large due to the short fluorescence lifetime of the dye.

We hope readers will find this tutorial accessible and useful. Those who need more resources or want to deepen their knowledge of basic concepts of fluorescence are encouraged to read the textbooks by J. R. Lakowicz [8], B. Valeur and M. Berberan-Santos [9], and D. Jameson [16].

Acknowledgments

This work was supported by the National Science Foundation (BIO-1918716). The author thanks Nikita Kumari for assistance in acquiring some of the data used to prepare figures, and all the members of her research lab for help proof-reading the article. The authors have declared that no conflicting interests exist.

References

- [1] J. Vangindertael, R. Camacho, W. Sempels, H. Mizuno, P. Dedecker, and K. P. F. Janssen, "An introduction to optical super-resolution microscopy for the adventurous biologist," *Methods Appl Fluoresc*, vol. 6, no. 2, p. 022003, 2018.
- [2] K. S. Grubetamayer, K. Yserentant, and D. P. Herten, "Photons in numbers out: perspectives in quantitative fluorescence microscopy for in situ protein counting," *Methods Appl Fluoresc*, vol. 7, no. 1, p. 012003, 2019.
- [3] E. Lerner, T. Cordes, A. Ingargiola, Y. Alhadid, S. Chung, X. Michalet, and S. Weiss, "Toward dynamic structural biology: Two decades of single-molecule forster resonance energy transfer," *Science*, vol. 359, no. 6373, 2018.
- [4] Y. M. Sigal, R. Zhou, and X. Zhuang, "Visualizing and discovering cellular structures with super-resolution microscopy," *Science*, vol. 361, no. 6405, pp. 880–887, 2018.
- [5] Y. Hong, J. W. Lam, and B. Z. Tang, "Aggregation-induced emission," *Chem Soc Rev*, vol. 40, no. 11, pp. 5361–88, 2011.
- [6] S. E. Braslavsky, "Glossary of terms used in photochemistry 3(rd) edition (iupac recommendations 2006)," *Pure Appl Chem*, vol. 79, no. 3, pp. 293–465, 2007.
- [7] L. Stryer, "Fluorescence energy-transfer as a spectroscopic ruler," *Annu Rev Biochem*, vol. 47, pp. 819–846, 1978.
- [8] J. R. Lakowicz, *Principles of fluorescence spectroscopy*. New York: Springer, 3rd ed., 2006.
- [9] B. Valeur and M. N. Berberan-Santos, Molecular fluorescence: principles and applications. Weinheim, Germany: Wiley-VCH Verlag GmbH & Co. KGaA, second edition. ed., 2013.
- [10] R. M. Clegg, *The History of Fret*, vol. 2006 of *Reviews in Fluorescence*, book section 1, pp. 1–45. Springer US, 2006.
- [11] E. M. S. Stennett, M. A. Ciuba, and M. Levitus, "Photophysical processes in single molecule organic fluorescent probes," *Chem Soc Rev*, vol. 43, no. 4, pp. 1057–1075, 2014.

- [12] C. Wurth, M. Grabolle, J. Pauli, M. Spieles, and U. Resch-Genger, "Relative and absolute determination of fluorescence quantum yields of transparent samples," *Nat Protoc*, vol. 8, no. 8, pp. 1535–1550, 2013.
- [13] U. Resch-Genger and K. Rurack, "Determination of the photoluminescence quantum yield of dilute dye solutions (iupac technical report)," *Pure Appl Chem*, vol. 85, no. 10, pp. 2005–2026, 2013.
- [14] A. M. Brouwer, "Standards for photoluminescence quantum yield measurements in solution (iupac technical report)," *Pure Appl Chem*, vol. 83, no. 12, pp. 2213–2228, 2011.
- [15] K. Rurack, Fluorescence Quantum Yields: Methods of Determination and Standards, pp. 101–145. Berlin, Heidelberg: Springer Berlin Heidelberg, 2008.
- [16] D. M. Jameson, *Introduction to fluorescence*. Boca Raton: CRC Press, Taylor & Francis Group, 2014.
- [17] N. J. Turro, V. Ramamurthy, and J. C. Scaiano, *Modern molecular photochemistry of organic molecules*. Sausalito, Calif.: University Science Books, 2010.
- [18] A. K. Gaigalas and L. L. Wang, "Measurement of the fluorescence quantum yield using a spectrometer with an integrating sphere detector," *J Res Natl Inst Stan*, vol. 113, no. 1, pp. 17–28, 2008.
- [19] C. Wurth, C. Lochmann, M. Spieles, J. Pauli, K. Hoffmann, T. Schuttrigkeit, T. Franzl, and U. Resch-Genger, "Evaluation of a commercial integrating sphere setup for the determination of absolute photoluminescence quantum yields of dilute dye solutions," *Appl Spectrosc*, vol. 64, no. 7, pp. 733–741, 2010.
- [20] M. G. Rockley and K. M. Waugh, "The photoacoustic determination of fluorescence yields of dye solutions," *Chem Phys Lett*, vol. 54, no. 3, pp. 597–599, 1978.
- [21] M. Fischer and J. Georges, "Fluorescence quantum yield of rhodamine 6g in ethanol as a function of concentration using thermal lens spectrometry," *Chem Phys Lett*, vol. 260, no. 1-2, pp. 115–118, 1996.
- [22] J. H. Brannon and D. Magde, "Absolute quantum yield determination by thermal blooming fluorescein," *J Phys Chem*, vol. 82, no. 6, pp. 705–709, 1978.
- [23] M. J. Adams, J. G. Highfield, and G. F. Kirkbright, "Determination of absolute fluorescence quantum efficiency of quinine bisulfate in aqueous-medium by optoacoustic spectrometry," *Anal Chem*, vol. 49, no. 12, pp. 1850–1852, 1977.
- [24] S. R. Meech and D. Phillips, "Photophysics of some common fluorescence standards," Journal of Photochemistry, vol. 23, no. 2, pp. 193 – 217, 1983.

- [25] J. W. Hofstraat and M. J. Latuhihin, "Correction of fluorescence-spectra," *Appl Spectrosc*, vol. 48, no. 4, pp. 436–447, 1994.
- [26] D. Pfeifer, K. Hoffmann, A. Hoffmann, C. Monte, and U. Resch-Genger, "The calibration kit spectral fluorescence standards a simple and certified tool for the standardization of the spectral characteristics of fluorescence instruments," J Fluoresc, vol. 16, no. 4, pp. 581–587, 2006.
- [27] C. A. Parker and W. T. Rees, "Correction of fluorescence spectra and measurement of fluorescence quantum efficiency," *Analyst*, vol. 85, no. 1013, pp. 587–600, 1960.
- [28] P. C. DeRose, "Standard guide to fluorescence instrument calibration and validation," Report 7458, 2008.
- [29] M. Kubista, R. Sjoback, S. Eriksson, and B. Albinsson, "Experimental correction for the inner-filter effect in fluorescence-spectra," *Analyst*, vol. 119, no. 3, pp. 417–419, 1994.
- [30] M. Levitus, R. M. Negri, and P. F. Aramendia, "Rotational relaxation of carbocyanines comparative-study with the isomerization dynamics," *J Phys Chem*, vol. 99, no. 39, pp. 14231–14239, 1995.
- [31] M. E. Sanborn, B. K. Connolly, K. Gurunathan, and M. Levitus, "Fluorescence properties and photophysics of the sulfoindocyanine cy3 linked covalently to dna," *The Journal of Physical Chemistry B*, vol. 111, no. 37, pp. 11064–11074, 2007.
- [32] K. Suzuki, A. Kobayashi, S. Kaneko, K. Takehira, T. Yoshihara, H. Ishida, Y. Shiina, S. Oishic, and S. Tobita, "Reevaluation of absolute luminescence quantum yields of standard solutions using a spectrometer with an integrating sphere and a back-thinned ccd detector," Phys Chem Chem Phys, vol. 11, no. 42, pp. 9850–9860, 2009.
- [33] K. Rurack and M. Spieles, "Fluorescence quantum yields of a series of red and near-infrared dyes emitting at 600-1000 nm," Anal Chem, vol. 83, no. 4, pp. 1232–1242, 2011.
- [34] K. Nawara and J. Waluk, "Goodbye to quinine in sulfuric acid solutions as a fluorescence quantum yield standard," *Anal Chem*, vol. 91, no. 8, pp. 5389–5394, 2019.
- [35] D. Magde, R. Wong, and P. G. Seybold, "Fluorescence quantum yields and their relation to lifetimes of rhodamine 6g and fluorescein in nine solvents: Improved absolute standards for quantum yields," *Photochem Photobiol*, vol. 75, no. 4, pp. 327–334, 2002.
- [36] F. L. Arbeloa, T. L. Arbeloa, M. J. T. Estevez, and I. L. Arbeloa, "Photophysics of rhodamines - molecular-structure and solvent effects," *J Phys Chem*, vol. 95, no. 6, pp. 2203–2208, 1991.
- [37] I. L. Arbeloa and P. R. Ojeda, "Dimeric states of rhodamine-b," *Chem Phys Lett*, vol. 87, no. 6, pp. 556–560, 1982.

- [38] W. R. Ware, "Oxygen quenching of fluorescence in solution an experimental study of diffusion process," *J Phys Chem*, vol. 66, no. 3, pp. 455–458, 1962.
- [39] P. C. DeRose, "Recommendations and guidelines for standardization of fluorescence spectroscopy," Report 7457, 2008.
- [40] U. Resch-Genger and P. C. Derose, "Fluorescence standards: Classification, terminology, and recommendations on their selection, use, and production (iupac technical report)," *Pure Appl Chem*, vol. 82, no. 12, pp. 2315–2335, 2010.
- [41] U. Resch-Genger and P. C. DeRose, "Characterization of photoluminescence measuring systems (iupac technical report)," *Pure Appl Chem*, vol. 84, no. 8, pp. 1815–1835, 2012.